

NASA Contractor Report 3436

NASA
CR
3436
c.1

An Experimental Investigation
of a Large ΔP Settling Chamber
for a Supersonic Pilot Quiet Tunnel

Michael J. Piatt

CONTRACT NAS1-16096
JUNE 1981

NASA

TECH LIBRARY KAFB, NM
0061984



NASA Contractor Report 3436

An Experimental Investigation of a Large ΔP Settling Chamber for a Supersonic Pilot Quiet Tunnel

Michael J. Piatt
Systems and Applied Sciences Corporation
Hampton, Virginia

Prepared for
Langley Research Center
under Contract NAS1-16096



National Aeronautics
and Space Administration

**Scientific and Technical
Information Branch**

1981



TABLE OF CONTENTS

SUMMARY	1
SECTION 1 - INTRODUCTION.	3
LIST OF SYMBOLS	7
SECTION 2 - TEST FACILITY AND INSTRUMENTATION	8
SECTION 3 - METHOD OF DATA ANALYSIS	10
SECTION 4 - EXPERIMENTAL RESULTS AND DISCUSSIONS.	13
SECTION 5 - GENERAL COMMENTS AND RECOMMENDATIONS	34
SECTION 6 - CONCLUDING REMARKS.	39
REFERENCES.	41

SUMMARY

This report is a study of the flow quality in the settling chamber of a supersonic pilot quiet tunnel. The mean streamwise flow distributions and turbulence levels across the chamber were measured with a hot wire anemometer. Data were obtained downstream of a series of porous "Rigimesh" plates which have relatively large total pressure losses across them compared to more conventional "turbulence manipulators" such as honeycombs and screens. These porous plates are practical in supersonic blowdown tunnels where total pressure losses are not a limiting factor. Acoustic disturbances in the settling chamber, as the result of pipe and valve systems upstream, are a common problem in these facilities. The dense porous plates used in the pilot quiet tunnel settling chamber have been shown to be an effective means of reducing the chamber acoustic levels.

Information presented in this report reveals that these plates can produce nonuniform mean flow distributions downstream which result in the generation of large vorticity fluctuations. Several of the chamber components were removed one at a time (porous cone, porous plate, and steel wool) in an attempt to isolate the cause of the recorded mean velocity stratification. No explanation for this phenomenon can be presented with absolute certainty, due to the physical limitations on where data could be obtained in the facility. Some reasonable but somewhat speculative explanations are offered that may provide some insight to the problem. The

addition of a honeycomb downstream of the porous plates was not effective as a means of producing uniform mean flow. A perforated plate was installed in the chamber but it generated strong acoustic disturbances at discrete frequencies. It was determined that a series of screens with decreasing mesh size for the downstream screens was a most effective means of achieving the objective of a uniform mean flow distribution with reduced vorticity levels. Frequency spectra obtained across the series of screens show that they reduce vorticity over a wide frequency range for several different initial upstream vorticity conditions.

1. INTRODUCTION

Disturbance levels and mean velocity nonuniformities in wind tunnel settling chambers are of major interest because under some circumstances they have a direct effect on the flow quality in the test section. Vortical and acoustic disturbances generated upstream of the test section in low-speed tunnels are convected or propagated into the test section with changes in amplitude due only to the favorable pressure gradient associated with the contraction region unless additional attenuation devices are used. At high supersonic velocities the vorticity disturbances in well designed settling chambers have little effect on test section disturbances or on transition in the nozzle wall boundary layer due to the large expansion ratios of the mean flow. Data obtained by Anders et al.⁽¹⁾ at Mach 5 showed no measurable effect on free stream disturbances or nozzle wall boundary layer transition due to large changes in settling chamber velocity fluctuation levels. Boundary layer transition studies on a sharp cone in the free stream have been made by Laufer and Marte⁽²⁾. They varied the settling chamber velocity fluctuation levels from .6 percent to 7 percent over a range of test section Mach numbers from 1.7 to 4. Their results indicated that boundary-layer-transition Reynolds numbers on a cone model are affected by settling chamber disturbance levels below a Mach number of about 2.5 but there was no effect at higher Mach numbers.

It has long been established that pressure fluctuations radiated from the nozzle wall boundary layer are the dominate

disturbance mode in supersonic test facilities⁽³⁾. Hot wire measurements taken by this author in a Mach 5 rapid expansion nozzle, as well as data published by Anders et al.⁽¹⁾ in the same nozzle also indicate that acoustic pressure fluctuations radiated from the turbulent nozzle wall boundary layer are the primary disturbance in this nozzle and that vorticity levels are negligible. These data also show that in this nozzle at low Reynolds numbers where the nozzle wall boundary layer is laminar, the level of pressure fluctuations on the nozzle centerline are greatly diminished. Conceivably these reduced free stream disturbance levels can be influenced by acoustic disturbances originating upstream of the contraction, at least for low supersonic Mach numbers.

Nevertheless, a properly designed settling chamber is important to minimize free stream disturbances even for high Mach number flows. Typical minimum disturbance levels obtainable in a well-designed settling chamber, such as the JPL 20-inch tunnel, are less than 1 percent⁽⁴⁾. If a severe flow problem exists, such as separation along the settling chamber inlet diffuser, it can have a pronounced effect on the nozzle flow. Mabey and Sawyer⁽⁵⁾ found that this flow condition in the chamber resulted in fluctuations in angles of incidence and yaw in the working section, accompanying 1.3 percent velocity disturbances in the settling chamber for a tunnel Mach number of 3. Related effects have been found by Jones and Feller⁽⁶⁾ in Mach 6 flow and by Amick⁽⁷⁾ in a Mach 8 wind tunnel.

The use of various pressure drop devices to attenuate

acoustic and vortical disturbances may also have adverse effects on settling chamber disturbance levels. Lau and Baines⁽⁸⁾ have shown that large transverse variations in the mean streamwise velocity can be generated by curved screens with large values of K . This effect is similar to the refraction of light at a material interface; the streamlines are deflected towards the normal to the screen as they pass through it. The curvature of a screen placed in a uniform flow will produce a pressure drop that varies laterally with the angle of incidence of the upstream streamlines. The same lateral pressure distribution could be obtained from a planar device of nonuniform porosity placed in uniform flow. Some very relevant work done by Nagib^(9,10,11) and his associates at IIT has illustrated the ability to manipulate and control turbulence intensities in low-speed flow. The proper use of pressure drop devices such as screens and honeycombs can significantly dampen velocity fluctuations and force nonuniform velocity distributions to become more homogeneous.

This report is an investigation of the disturbance levels in the settling chamber for a supersonic pilot quiet tunnel. A hot wire anemometer was used to determine the mean flow and rms fluctuating velocities at several stations in the chamber. The effects of various turbulence manipulators (screens, honeycomb, porous plates and cones, and perforated plates) on these fluctuating levels are determined and frequency spectra are presented to aid the analysis.

Use of trade names or names of manufacturers in this report does not constitute an endorsement of such products or manufacturers.

The author would like to acknowledge the valuable technical assistance of Mr. William O. Moore, III who conducted tunnel operations and performed the computer programming for data acquisition.

LIST OF SYMBOLS

D	orifice diameter
K	pressure-drop coefficient, $\Delta P / (1/2) (\rho \bar{u}^2)$
M	Mach number
P	pressure
R	settling chamber radius
u	streamwise velocity
v	velocity through orifice
y	radial coordinate measured from chamber centerline
ω	resonant frequency measured in radians
ρ	density
γ	ratio of specific heats

Subscripts

o	settling chamber
---	------------------

Superscripts

-	long time average
~	root mean square

2. TEST FACILITY AND INSTRUMENTATION

The settling chamber shown in figure 1 is intended to produce low turbulence, uniform flow upstream of the nozzle contractions for a Mach 3 axisymmetric nozzle and a Mach 3.5 two-dimensional nozzle. The effort is part of an on-going project at NASA Langley to develop a "quiet" supersonic test facility where the level of nozzle wall radiated pressure fluctuations are to be reduced⁽¹⁾. A 0.64 cm thick porous "Rigimesh" cone is located at the inlet of the chamber. The large pressure drop across the cone prevents flow separation along the diffuser inlet section. The cone is followed by four approximately equally spaced 0.64 cm porous "Rigimesh" plates with steel wool packed between the first two plates. The purpose of the porous plates and steel wool is to dampen the upstream acoustic disturbances originating from the pipe system and control valves and to promote uniform mean flow due to the large pressure drop associated with the porous plates. The concept is practical for supersonic blowdown tunnels where pressure losses are not a limiting factor. The plates are followed by a series of seven screens with decreasing mesh size toward the nozzle, intended to suppress upstream vorticity. A vacant section exists between the plates and screens where additional turbulence manipulators or acoustic baffles can be inserted.

The chamber was fitted with a sonic nozzle with a throat radius of 5.08 cm. A Disa Model 55M10, constant temperature anemometer with a standard 1:20 ratio bridge was used to obtain

hot wire measurements across the chamber at instrumentation ports A, B, and D as shown in figure 1. The probe support system and the location of the ports limited the surveys to the horizontal plane only.

The wire composition was Platinum with 10 percent Rhodium. The wires were 2.5 μm in diameter with a typical length to diameter ratio of 200. The data were obtained from ensemble averages of the measured quantities consisting of pressure, temperature, mean wire voltage, and rms wire voltage readings taken over about a 25 second interval. This was accomplished with the use of a HP scanner, Model 3495-A, connected to a HP voltmeter, Model 3455-A, monitored by a HP 9845-T calculator. The calculator was programmed to analyze the data as described in the next section. In addition, the hot wire signal was processed by a HP spectrum analyzer, Model 3582-A, this information was input to the calculator to obtain a permanent record of the frequency content at each probe location.

3. METHOD OF DATA ANALYSIS

Expedient data reduction was possible with the aid of the computer. This capability can produce a more accurate representation of the flow parameters by allowing data based correction factors to be directly applied to the measured quantities. This method was used for both hot wire calibration and data acquisition in the chamber.

Each wire was individually calibrated in the settling chamber itself over the range of Reynolds numbers for which data would be obtained. With sonic flow at the throat and measured local values of pressure and temperature, the mass flow through the chamber can be calculated with the added assumptions that the flow is uniform and isentropic and the boundary layer thickness at the throat is negligible. The calibrations were done on the chamber centerline at instrumentation port B, shown in figure 1. An average local boundary layer displacement thickness was computed, at the measured temperature and pressure, for a smooth flat plate assuming minimum and maximum turbulent boundary layer growth lengths from the last screen and from the last "Rigimesh" plate, respectively. Based on this thickness, an estimate of the flow area was obtained, where the streamwise velocity was assumed to be uniform. Later measurements taken across the chamber at port B showed the mean streamwise velocity to be uniform within 3 percent at all Reynolds numbers and the actual boundary layer thickness to be in good agreement with the calculated value. Any error associated with this technique would be manifested as a small shift in the absolute mean velocity

levels but would have no bearing on the relative levels between the measured quantities. Variations in Reynolds number, over which the wire was calibrated, were primarily due to changes in density rather than velocity. For the present test conditions, a simple King's law relationship defined the wire's response very well. A typical calibration curve, showing the linear relationship between the wire voltage squared and the square root of the product of density and velocity, is shown in figure 2. As part of the calibration procedure the frequency response of the wires was determined. From the square wave test, the cut-off frequency was found to be nearly 50 kHz in the chamber flow of 6.1 m/sec at an overheat ratio of 0.7. The square wave technique for determining frequency response has accuracy limitations associated with judgment involved in determining the damping coefficient from the experimental response and also due to the influence of the higher order terms on the output wave form. To obtain a more reliable frequency cut-off, a sine wave was applied to the external test jack on the anemometer to measure the frequency response directly. This method was investigated by Bonnett and Roquefort⁽¹²⁾ and found to be in good agreement with the response obtained by directly heating the wire with an external source. A typical wire frequency cut-off using this method was about 70 kHz with slight variations associated with the stagnation pressure in the chamber.

To obtain the fluctuating flow quantities, the wire sensitivity was determined from the local derivative of the product of density and velocity with respect to voltage at the mean

values. The rms voltage was related to the product of density and velocity fluctuations by this sensitivity.

For comparison with pressure transducer measurements, the rms voltage was assumed to be the result of acoustic disturbances originating from a simple plane wave traveling down the chamber. Although it is recognized that this assumption is not physically correct, since there is vorticity in the flow, it does provide an approximate method of separating the density fluctuations from the velocity disturbances. The use of this assumption then gives the relationship⁽¹³⁾,

$$\frac{d\rho}{\bar{\rho}} = M \frac{du}{\bar{u}} \quad (1)$$

from which it can be seen that the velocity fluctuations are much larger than the density contribution to the total normalized rms quantity at the Mach number in the chamber of about 0.017. Therefore, assuming the flow to be incompressible and all of the disturbances to be velocity fluctuations can result in a maximum error of about 2 percent. The precise error is dependent upon the relative magnitude of the acoustic disturbances, resulting in density and velocity fluctuations, and vorticity composed of only velocity fluctuations.

The large pressure drop across the various components used as acoustic baffles and turbulence manipulators for several combinations of tunnel components is shown in figure 3. Hot wire data were obtained for each of these test conditions over the range of stagnation pressures that correspond to the mass flow rates shown in the figure.

4. EXPERIMENTAL RESULTS AND DISCUSSION

Measurements With All Components Installed

Hot wire measurements made in the described settling chamber indicate that a serious problem exists in this facility. The mean streamwise velocity profiles obtained upstream of the screens at port A are extremely nonuniform as shown in figure 4. The calculated average velocity is about 6 m/sec. There is a large velocity deficit along the chamber centerline and a corresponding increase in the streamwise velocity as the radial distance increases. This behavior was recorded at a series of stagnation pressures from 310 to 827 kPa. The flagged symbols were obtained on the other side of the centerline and suggest that this flow pattern is symmetric. Some evidence of the boundary layer is apparent yet it is considerably thinner than anticipated.

The corresponding turbulence intensities are shown in figure 5. These measurements were obtained with a single hot wire and represent only the streamwise fluctuations normalized by the local mean values. The centerline levels are as high as 16 percent of the local stream velocity. There is considerable variation with stagnation pressure but no consistent trends are apparent. The turbulence intensities, like the mean velocities, are nearly symmetric about the centerline of the chamber. The wide variation of \tilde{u}/\bar{u} is misleading due to variations in the normalizing quantity \bar{u} . The actual values of \tilde{u} are between .2 and .6 m/sec across the chamber.

Downstream of the screens at instrumentation port B, the mean velocity profiles and the \tilde{u} fluctuations have changed con-

siderably as shown in figures 6 and 7. The time-averaged velocity is now uniform at all stagnation pressures on both sides of the centerline due to the effects of the seven screens operating on the flow over several chamber diameters of streamwise distance. The boundary layer thickness has increased with profile shapes that resemble what one would expect to find at these Reynolds numbers. The edge of the boundary layer is located at $y/R \approx .85$ so the boundary layer thickness $\approx .15R$.

The corresponding turbulence intensities (figure 7) have decreased in the center region and exhibit less variation over the pressure range investigated. In general it can be said that the lateral communication that the flow experienced as it passed through the screens, resulting in greatly accelerated mean streamwise velocity along the centerline, had a significant damping effect on the local turbulence levels. In contrast, the process associated with decelerating the flow around the circumference of the chamber as it passed through the screens had only a nominal effect on the corresponding \tilde{u} fluctuations. An analogy can be made with the difference between flow through a nozzle and a diffuser. A favorable streamwise pressure gradient suppresses turbulence while an adverse gradient usually will increase turbulence levels.

The peaks in the turbulence profiles located near $y/R = .65$ (figure 7) are believed to be the result of large scale vorticity originating from the shear layer in the mean velocity that existed upstream. This vorticity shows some Reynolds number dependence. Lower stagnation pressures resulted in more

attenuation of the \tilde{u} fluctuations across the screens. The increase in turbulence near the wall at port B is the result of vorticity in the turbulent boundary layer and is not simply due to the decrease in the normalizing quantity \bar{u} . The boundary layer edge is near $y/R = .85$ yet the quantity \tilde{u}/\bar{u} decreases as $y/R \rightarrow .95$ then \tilde{u}/\bar{u} begins to increase. This inflection point in the \tilde{u}/\bar{u} curve is dependent on both the boundary layer vorticity and the decreasing time-averaged velocity.

The one percent velocity fluctuations present on the chamber centerline at port B (figure 7) are believed to consist partly of residual acoustic disturbances that originated far upstream in the pipe system and control valves and were passed by the series of porous plates. These disturbances would be nearly homogeneous across the chamber, assuming no standing wave patterns, and would be virtually unaffected by the screens or mean velocity stratification. These assumptions allow the reduction of velocity disturbances to normalized rms pressure fluctuations from the equation⁽¹³⁾,

$$\frac{\tilde{p}}{\bar{p}_0} = \gamma M \frac{\tilde{u}}{\bar{u}} \quad (2)$$

The levels of \tilde{u}/\bar{u} may then be compared with pressure data obtained with flush wall mounted transducers which respond only to acoustic disturbances. This comparison is shown in figure 8 along with some pressure transducer data from the Mach 5 pilot quiet tunnel settling chamber (ref. 14). The pressure

fluctuations derived from the hot wire data on the centerline are appreciably higher than the levels obtained from the flush mounted transducers. This may be due to the accuracy limitations of the two independent measuring devices or may in fact be an indication of the vortical disturbances on the chamber centerline superimposed on the acoustic field. Spectral analysis of both types of data tends to indicate that vorticity does account for the higher levels detected by the hot wire. Thus, it may be concluded by application of equation (2) to the pressure data of figure 8 and comparison of the resulting values of \tilde{u}/\bar{u} with the hot-wire data, that roughly one-half of the measured rms velocity fluctuations are acoustic disturbances. Figure 8 also illustrates that the acoustic baffles installed in the chamber reduced the noise level to less than 10 percent of the initial empty chamber values.

To determine if additional vorticity introduced at port A had any effect on the disturbance levels at port B, a .9 cm diameter rod extending to $y/R = .5$ beyond the centerline was placed in port A. This rod diameter was used because a thermocouple of equal diameter will be used in the chamber for temperature measurements during tunnel operation. Any vorticity caused by eddy shedding from the rod was not detected downstream at port B. The measured velocity fluctuations are shown in figure 9 for a stagnation pressure of 586 kPa. The solid symbols represent the disturbances when the rod was upstream. Similar behavior was observed over a range of pressures. It may be concluded that the \tilde{u} fluctuations already present at port

A dominate the downstream values and any effects of added vorticity from the rod are secondary.

Spectrum

An examination of the spectral components from the hot wire response can provide additional information about the sources of disturbances. As described in the method of data analysis, the nonlinear wire response was matched by a fourth-order polynomial stored in the computer. It was therefore not practical to relate the real time wire response, measured in volts, to instantaneous velocity fluctuations. The spectra derived from the wire time signal are expressed in rms volts/ $\sqrt{\text{Hz}}$ and show only the relative magnitudes of energy associated with each frequency interval. The spectrum analyzer divides the pre-set frequency range into 256 equal bandwidth segments. The signal amplitude in a given frequency interval is dependent upon this bandwidth and therefore dependent on the frequency range selected. In order to obtain consistent results for different range settings, the amplitude levels are normalized by dividing the values in each interval by the square root of the bandwidth of an ideal rectangular filter with cut off frequencies equal to the interval size. The rms voltage is computed on a point-by-point basis, for each of the 256 frequency intervals, from 8 independent spectra obtained at a given probe location and at a constant chamber pressure. All the spectra presented here were obtained by this procedure. The power spectra are related to the square of the magnitudes shown on the plots.

Electronic noise, inherent to all hot wire systems, can

be a source of error in the determination of the rms velocity fluctuations. In the present data the measured rms electronic noise levels were always more than an order of magnitude less than the minimum rms disturbance levels recorded in the chamber. A typical spectra obtained at port B near the maximum disturbance coordinate is shown with a log amplitude scale in figure 10. It is apparent that nearly all of the energy is below 10 kHz and that the electronic noise adds an insignificant contribution to the overall signal level below this frequency. To show adequate detail in the following discussion, the spectra are presented on a linear scale and extended only to 10 kHz frequency.

The two spectra shown in figures 11 and 12 were obtained on the chamber centerline at the upstream location, port A, and downstream of the screens at port B, respectively. There are a set of well-defined peaks in the spectra at port A (fig. 11) which are significantly reduced or eliminated as the flow passes through the screens as shown by comparison with figure 12. The screens are relatively low pressure drop devices and would have little effect on acoustic disturbances except at frequencies greater than 400 kHz. The reduction in spectral energy across the screens is therefore associated with vortex structures at port A which are broken up and dissipated by viscous interactions. The narrow-band peaks in the spectrum at port B (fig. 12) may be some residual vorticity that would account for the discrepancy between the centerline hot wire measurements expressed as pressure fluctuations from equation

(2) and the pressure fluctuations due to the acoustic field obtained with a flush wall mounted transducer at port B (fig. 8).

At port B there is a dramatic increase in the rms level from the centerline to $y/R = .67$ (fig. 7). The corresponding spectral energy also increases. Figure 13 shows a comparison of time signal traces recorded from the hot wire on the centerline and at $y/R = .67$. Both signals were high pass filtered at 20 Hz. Although the scale of the disturbances is greatly increased, the effects of the screens on the upstream vorticity is consistent with the centerline data. Figures 14 and 15 shows the spectra for $y/R = .67$ at ports A and B, respectively. Although it is not apparent on the figures due to the linear scale, as the flow passes through the screens there is an appreciable decrease in the energy content at the very low frequencies, the peak at 40 Hz is reduced from 445 mV to 250 mV. These low frequencies are associated with relatively large scale structures which are broken up by the screens resulting in smaller scale disturbances at port B. These smaller scale disturbances account for the actual increase in the spectral energy at the higher frequencies from port A to port B.

Spectra were also obtained in the wall boundary layer upstream and downstream of the screens. The flow in this region is obviously subject to the boundary condition at the wall and as a result, the scale of the vorticity is believed to be smaller than that associated with the large shear layer in the free stream. The two spectra from ports A and B at $y/R = .975$ are

shown in figures 16 and 17, respectively. There is a reduction in the energy level over the entire frequency range as the flow passes through the screens at this radial location. The significant attenuation of the high frequency components downstream may be due to the actual elimination of some of the smaller scale vorticity due to the viscous effects of the screens.

Removal of Porous Cone

In an effort to identify the source of the mean streamwise velocity nonuniformities that exist in the chamber at port A, some tests were conducted in an attempt to determine which components upstream of port A may be responsible for the problem. The purpose of the "Rigimesh" cone at the chamber inlet is to force the incoming jet to attach to the wide angle diffuser section allowing the flow to pass through the cone uniformly over its entire cross section. Diffuser technology is complex, making accurate predictions of the actual downstream flow conditions difficult. It was reasoned that the porous cone may be contributing to the irregular mean velocity distributions downstream, so it was removed from the chamber. As a result, the incoming jet impinges upon the porous flat plate downstream of the cone location. For safety reasons, tests under these conditions were limited to a stagnation pressure of 310 kPa.

The resulting mean velocity profiles at port A with the cone removed from the chamber are shown in figure 18, along with the data obtained at the same pressure in the complete chamber. There is little change in the mean streamwise velocity profile.

The four remaining porous plates and the steel wool apparently determine the mean velocity distributions downstream. The corresponding rms velocity fluctuations are shown in figure 19. The turbulence level increases caused by the removal of the cone are probably due to the higher initial turbulence at the upstream porous plate as a result of the mixing layer associated with the incoming jet.

Downstream of the screens at port B, the conclusions are similar as indicated by figures 20 and 21. The mean velocity is more uniform and the streamwise turbulence levels are diminished compared with those at port A. The screens had a most pronounced effect on the centerline velocity fluctuations which were reduced from 19 percent to about 1.5 percent while the mean normalizing velocity was doubled. The velocity fluctuations at port B increase to a maximum near $y/R = .5$ which is about the center of the shear layer in the mean velocity that exists upstream. In general, the viscous mixing effects caused by the screens are consistent for two different upstream turbulence distributions. The differences in the upstream turbulence distributions are similar to the differences in the curves at port B even though the general shape of the curves has changed considerably from the data obtained upstream of the screens.

Removal of the Downstream Porous Plate

The fact that the mean velocity profiles were not changed significantly by removal of the porous cone indicates that the problem is caused by the series of porous plates or the steel wool between them. The cone was reinstalled in the chamber and

the downstream porous plate, closest to the screens, was removed. The results of the mean velocity and turbulence surveys at port A are shown in figures 22 and 23, respectively. The data are presented across the entire chamber because the profiles are not symmetrical about the centerline. Comparison with figure 4 indicates that this plate had a strong effect on the mean velocity distributions recorded at port A. One side of the chamber exhibits more uniform mean velocity than before. The boundary layer flow on the lower velocity side of the chamber is irregular, which may be the result of flow around, rather than through the porous plates. There was a small gap between the three upstream porous plates and the chamber wall through which some flow can pass. This mass flow could be significant due to the large pressure drop across the plates. Only the last porous plate, removed for these tests, was welded in place to seal the chamber. The turbulence intensities at port A (fig. 23) are generally less than the values measured in the complete chamber (see fig. 5). These reduced levels represent an overall improvement in the stilling chamber at port A that is also expected to be present downstream of the screens.

Measurements obtained at port B do show an improvement, as seen by comparison of figures 24 and 25 with figures 6 and 7. The mean velocity profiles are flat and nearly uniform except for some localized variations which coincide with the location of the peak velocity at the upstream station. The turbulence levels at station B are less than 2 percent over most of the chamber diameter, however, the levels in the center regions to

$y/R \approx .35$ are increased somewhat. The higher disturbance intensities around the circumference of the chamber are due only in part to the reduction of the normalizing mean velocity in the boundary layer. This streamwise turbulence increase extends from the wall to $y/R = .75$ but the boundary layer thickness is less than half this distance.

Porous Plate Investigation

The affect of the downstream porous plate on the flow quality at port A was significant. The removal of this plate from the chamber resulted in a change in "initial upstream conditions" now apparently determined primarily by the next upstream porous plate still in place in the chamber. In addition, the removal of the downstream plate increased the streamwise mixing length from the plates to port A by about two-thirds of a chamber diameter. If the porosity of the porous plates is not uniform over their cross-sectional area this would certainly effect the mean streamwise flow distribution downstream, due to the large average pressure drop across the plates as shown in figure 3.

An independent "bench" test was conducted to determine the local porosity of the downstream plate which was removed from the tunnel. The mass flow through the plate was determined at several radial locations as a function of the total pressure difference from one side of the plate to the other. This was accomplished by fitting the upstream side of the plate with a rubber seal which covered its entire area except for a 2.22 cm hole which allowed the air to pass through the porous material

at a single radial location. The concave side of the plate was pressurized and the total mass flow through the hole in the seal was obtained by recording the mass flow required to maintain a constant pressure differential across the plate. The opening in the rubber seal was then moved to a different location on the plate and the test was repeated.

The results shown in figure 26 are typical of the data generated around the circumference of the plate at various radial coordinates. The mass flow has been adjusted to correspond with the total mass flow through the plate at a given ΔP if the porosity was uniform and equal to the measured local value. The mass flow range shown in figure 26 corresponds to the tunnel mass flow rates for chamber pressures from about 300 to 850 kPa. From these data it is apparent that the porosity of this plate is not uniform over its area. There is a trend of more mass flow through the center of the plate than around the periphery at a given differential pressure. This result appears to be just the opposite of trends indicated by the measured velocities at port A when this plate was in the chamber, as shown in figure 4. The apparent discrepancy probably indicates that downstream velocities are determined by overall net effects of all the porous plates and cone acting as a unit.

Addition of Honeycomb-Screen Combination

When the problems previously discussed here were identified, emphasis was shifted to the determination of a quick inexpensive solution that would result in acceptable flow in the chamber, so that the nozzle investigation could proceed. Having improved

the flow by the removal of one porous plate, it was decided to operate on this existing flow condition to try to bring the streamwise velocity fluctuations to acceptable levels at the nozzle inlet, rather than removing the other plates and the steel wool to isolate the cause of the problem. It has already been shown (fig. 8), that the porous plates act as effective acoustic baffles and redesigning the entire chamber was not a practical solution.

A honeycomb with cells that were 0.95 cm across and a length of 10 cm was installed in the chamber downstream of instrumentation port A. The downstream side of the honeycomb was located 21.6 cm in front of the first screen. An additional screen (30 mesh) was secured to the downstream side of the honeycomb as recommended in reference 9. In addition, the leak around the porous plates was sealed to block the flow passage around the plates.

Measurements at port A were repeated and showed that the leak around the plates, believed to be a possible cause of the irregular flow in figures 22 and 23, actually had little effect on the flow at this location. The velocity profiles at port B are shown in figures 27 and 28. Comparison with figures 24 and 25 show the mean velocity profiles are less uniform than before the addition of the honeycomb screen combination, while there is some increase in the streamwise rms velocity fluctuations, particularly at the two highest pressures. The honeycomb was only 23 cell distances upstream of the first damping screen which was probably too close to allow sufficient decay of non-uniformities in mean velocity and turbulence generated by the

honeycomb⁽⁹⁾. Also, the attachment around the periphery of the honeycomb with its support ring was not satisfactory with some damaged and blocked cells which probably contributed to the increased turbulence for $y/R > .75$ shown in figure 28.

Additional data were obtained further downstream at instrumentation port D to determine if the increased decay and mixing length would result in more uniform flow. The plots are shown in figures 29 and 30. The limited amount of data obtained at this location indicates that the local mean velocity nonuniformities may be partially preserved downstream. The turbulence intensities have decreased to about .7 percent of the mean values on the centerline but begin to increase beyond the radial distance $y/R = .5$ reaching 3.3 percent of the mean velocity near the chamber wall. Although the nozzles are designed to remove the turbulent boundary layer by suction upstream of the throat, it is yet to be determined if the favorable pressure gradient leading into the nozzle will sufficiently dampen the high turbulence levels near the chamber wall and reduce the boundary layer thickness enough to make this suction an effective means of preventing settling chamber influences in the test section, or on the nozzle wall boundary layer.

Addition of a Perforated Plate

The mean streamwise velocity profiles at port A have shown various degrees of nonuniformity for each of the test conditions presented so far. The vorticity resulting from this shear layer in the mean flow has had an adverse effect on the turbulence levels downstream. The installation of a perforated plate with

equal hole sizes and hole spacings upstream of port A might be expected to improve the uniformity of the mean flow far downstream provided that the pressure drop across the plate is large enough. The open to closed area ratio of the perforated plate must be such that the mean streamwise flow is forced to accelerate to many times its average upstream velocity as it passes through the openings in the plate.

With these ideas in mind, a perforated plate with holes .953 cm in diameter and an open area to total surface area ratio of .05 was placed in the chamber in the location of the downstream porous plate which was removed in an earlier test. The honeycomb was removed from the chamber because it degraded the flow quality, however, the extra screen (30 mesh) on the downstream side of the honeycomb was left in place for this investigation. The perforated plate was .635 cm thick aluminum and was flat rather than concave like the porous "Rigimesh" plates. The total pressure loss in the chamber when this plate was installed is shown in figure 3. The pressure drop across the perforated plate alone is nearly twice the pressure drop across one of the porous plates.

Hot wire data obtained at port B with the perforated plate upstream showed the \tilde{u}/\bar{u} fluctuations ranged from 2.5 percent to 4 percent across the center core of the chamber extending to $y/R = .5$. The data obtained with the downstream porous plate removed (fig. 25) show turbulence levels around 2 percent near the chamber centerline at port B. Most of the increase in the fluctuating velocity with the perforated plate installed

is associated with the presence of a sharp resonance peak in the hot wire spectra at 11,700 Hz. A spectral plot obtained on the chamber centerline at port B is shown in figure 31. An increase in the amplitude at the harmonic frequency of about 24 kHz is also apparent. It is believed that these peaks are due to acoustic disturbances generated from the eddy shearing off the sharp corners of the holes in the plate. These "edge tones" result in a Strouhal number $\frac{\omega D}{V}$ of 5.6, where the velocity through each orifice is about 122 m/sec. It was considered likely that this high frequency sound would have a negative effect on the nozzle flow, so the perforated plate was removed from the chamber. Another factor that probably contributed to the increased turbulence at port B was the very high solidity of 0.95 for the perforated plate. Previous research⁽⁹⁾ has shown that such high solidity components can introduce additional vorticity that may persist for very large downstream distances and could presumably affect the flow downstream of damping screens.

Independent Orifice Plate Investigation

The tendency of a perforated plate to generate acoustic pressure disturbances at discrete frequencies makes it unattractive as a turbulence manipulator in settling chamber applications. An independent test program was conducted on an orifice plate to determine the effects of upstream and downstream bevels on the generation of acoustic disturbances. Data from several orifice plate-screen combinations are included.

The plate was .635 cm thick aluminum and the minimum

diameter of the orifice was .476 cm. An 82° included angle bevel approximately 0.15 cm deep was machined into the orifice plates for the series of convergent and divergent nozzle tests. Pressurized air was passed through the orifice plates and exhausted to the atmosphere. Acoustic levels were measured over a range of throat velocities with a sound level meter made by Audio Dynamics (model SLM-100) placed downstream of the orifice about 15 cm from the exit, at such an angle that it was not directly exposed to the jet flow.

The results are summarized in table 1. The background noise level, with no flow through the orifice, was 67 dB. From these results it is clear that case 1, the straight orifice, is quieter than the convergent and divergent entries and their combination, (cases 2-4). The flow is obviously separated on the downstream side of the beveled orifices (cases 2 and 4) at these velocities due to the 82° included angle expansion. It is not clear, however, why this resulted in noise levels that are higher than those recorded from the straight orifice where the flow is also separated on the downstream side. Perhaps the bevels were not machined accurately and introduced a slight asymmetry which had adverse effects on the flow through the orifices.

The output from the sound meter was connected to a spectrum analyzer to determine the frequency content of the signal. The spectra that corresponds to case 1 at a velocity of 61 m/sec is shown in figure 32. There is a sharp peak in the amplitude spectra at 3.2 kHz. This resonant frequency

yields a Strouhal number of 1.6. Several additional peaks, containing less energy at higher frequencies than the resonance, are also apparent on the figure. These spikes may be harmonics of the natural frequency generated by the flow through the orifice. Cases 2 and 3 produced nearly identical spectra at a velocity of 61 m/sec and, similarly, the recorded acoustic levels are the same for the two cases. The spectra for case 3, shown in figure 33, has considerably more energy at the 3.2 kHz resonant frequency than the straight orifice case measured at the same velocity. It is interesting to note that the peaks in the rest of the spectra occur at the same frequencies as the straight orifice case, figure 32, but the magnitudes of these higher frequency components have not increased proportionally with the change in amplitude of the resonant frequency.

The remaining entries in table 1, cases 5-15, investigate the influence of screen on the generation of acoustic disturbances as the result of flow through several orifice plate geometries. In general, the addition of these screens had favorable effects. The lowest noise level of all cases investigated resulted from placing a 50 mesh screen on each side of a straight orifice, listed as the seventh entry in table 1. The spectra that corresponds to case 7 at a velocity of 61 m/sec is shown in figure 34. The amplitude at the natural frequency of this system (3.2 kHz) is the same value as the peak at the resonant frequency in the spectra resulting from the straight orifice case without screens shown in figure

32. In comparing these two spectra, it is apparent that the peaks at frequencies above the resonance occur at the same locations along the frequency axis. The effects of the screens were to attenuate these higher frequency components.

Screens placed against the beveled orifice plates resulted in a decrease in the recorded acoustic disturbances. Like the straight orifice, the reduction was primarily due to a decrease in the higher frequency components and there was little change in the resonant frequency amplitude with the addition of screens. Cases 14 and 15 involve the use of a 30-mesh screen on a straight orifice. There were no significant differences noted between the two different mesh size screens used against the straight orifice.

Removal of Steel Wool From Settling Chamber

Although the independent orifice plate investigation showed that the acoustic disturbance levels generated by a perforated plate could be reduced by placing screens against the plate, the peak noise amplitude occurring at the resonant frequency could not be changed by this method. Based on these findings, no further attempts to use a perforated plate in the chamber were considered. The problem of nonuniform mean velocity profiles downstream of the porous plates persisted. These skewed velocity profiles have to be linked to the three remaining porous "Rigimesh" plates and the steel wool between them, see figure 1. It is possible that the steel wool was packed between the plates in such a manor that its density was not homogeneous in the plane perpendicular to the chamber flow. The total pressure

losses associated with the steel wool are significant. Figure 3 shows the total pressure drop across the chamber with the steel wool and the downstream porous plate removed from the chamber. The pressure losses associated with the steel wool are equivalent to the combined losses of more than three of the porous plates. Slight nonuniformities in its porosity could be detrimental to the chamber flow.

The steel wool was removed from the chamber to determine its effect on the mean flow downstream. The results obtained at port B were puzzling. The flow exhibited extremely unsteady behavior and hot wire measurements were difficult to repeat. Initial data indicated that the mean velocity was less uniform than expected downstream of the screens and that the turbulence levels were between 1 percent and 2.5 percent across the chamber. Distributions of the mean velocities are shown in figure 35 and the initial turbulence measurements are shown as the flagged symbols in figure 36. In contrast to all other data at port B presented in this report, the highest turbulence levels are on the chamber centerline and the fluctuating streamwise velocity decreases with increasing radial distance. Data obtained a couple days later (unflagged symbols in fig. 36) showed that the \tilde{u}/\bar{u} fluctuations had jumped to nearly 8 percent at $y/R \approx .85$ with decreasing turbulence levels on both sides of this point.

There is no explanation for this observed behavior at this time. Continued measurements, not shown on figure 35, recorded mean velocity variations of nearly 50 percent across

the chamber, downstream of the screens at port B. Prior to the removal of the steel wool all of the data presented in this report was repeatable and believed to be accurate. There were no changes made in the experimental procedures or data acquisition equipment before measurements were obtained in the chamber with the steel wool removed. It is believed that the observed discrepancies in the fluctuating streamwise velocities shown in figure 36 are related to some change that took place in the flow between the two sets of measurements.

5. GENERAL COMMENTS AND RECOMMENDATIONS

Porous Plates

The proper design of settling chambers for supersonic blow down tunnels involves careful consideration of turbulence manipulators to assure good flow quality at the nozzle inlet. Facilities such as the supersonic pilot quiet tunnel usually involve complex valving arrangements and considerable plumbing before the flow enters the settling chamber to assure adequate air temperature and pressure control. Acoustic disturbances originating from the upstream pipe system and valves are preserved as the flow enters the settling chamber. The first problem encountered in settling chamber design of this nature is the reduction or elimination of these acoustic disturbances. This was accomplished in the pilot quiet tunnel settling chamber by using a series of porous "Rigimesh" plates with a large pressure drop across them. The results shown in figure 8 illustrate that they are an effective means of reducing inlet acoustic levels. This investigation revealed, however, that these porous plates have a negative side effect. They may produce nonuniform mean flow downstream which results in the generation of large scale vorticity associated with this shear layer in the mean streamwise flow.

The pressure losses in the chamber due to the turbulence manipulators are shown in figure 3. The isolated characteristics of one porous plate can be observed by comparing the curve in figure 3 that represents the pressure losses in the complete chamber with the data points obtained in the chamber when one

of the plates was removed. The mean velocity downstream of the porous plate in the chamber is nearly constant for all mass flow rates. This velocity is related to the ratio of the cross-sectional area of the nozzle throat and the cross-sectional area of the chamber itself, with small corrections due to boundary layer thickness variations at different stagnation pressures. A porous plate can be thought of as a perforated plate with a large number of very small openings spaced closely together such that the open to closed area ratio of the plate in the plane perpendicular to the streamwise flow will result in a total pressure drop equal to the measured pressure drop across the porous plate. This analogy allows an estimation to be made of the velocity through the plate. Based on the pressure losses shown in figure 3, a simplified one dimensional inviscid analysis (and therefore assuming the velocity coefficient of each orifice in the plate to be unity) yields an exit velocity of about 76 m/sec. A 5 percent variation in this exit velocity over the surface of the plate would be a magnitude equal to about 65 percent of the decelerated mean streamwise chamber velocity. Thus, it is apparent that the problem of mean velocity stratification across the chamber downstream of the porous plates may be the result of rather small variations in the porosity of the individual plates. It follows that the attachment of the porous plates to the support rings should not block any flow areas of the plates. The first three plates downstream of the cone (fig. 1) were fastened to the support ring with 12 tabs spaced evenly around the periphery of the plates.

The tabs were 3.2 cm (1.25 in.) wide by 1.3 cm (0.5 in.) thick and were welded to the porous plates such that about 8.5 cm² (1.3 in.²) of the porous area next to the inside wall of the support ring was completely blocked at each tab location. While insufficient data are available to determine if these blocked areas contributed to downstream nonuniformities in mean or fluctuating flow, it is believed that such effects were probably present. Clearly, the method of support for the porous plates should be improved to eliminate any large blocked areas.

The discussion so far has assumed that the flow at the exit of the porous plates is one-dimensional in the direction parallel to the chamber centerline. The porous plates used in this facility are semispherical to reduce the material stresses enough to withstand the loads at high stagnation pressures, up to 4000 kPa. They are placed in the chamber such that the convex side faces downstream. As mentioned in the introduction, there is some evidence (ref. 8) that this curvature will cause the flow to deflect as it passes through the plate, exiting the plate with a velocity vector inclined towards the perpendicular to the surface. This outward deflection of the mean flow would result in increased streamwise velocity around the circumference of the chamber downstream of the plate. This phenomena could be investigated by placing the downstream porous plate in the chamber such that its concave side faced downstream. If the curvature of the plates is the cause of the mean velocity nonuniformities then a honeycomb

placed directly downstream of the last porous plate would probably be an effective flow straightener, provided the total velocity entering each honeycomb cell was of nearly the same magnitude.

Screens

The actual mechanism, or combination of circumstances, that produced the mean velocity nonuniformities at port A is not known at this time. It is easy to understand that such problems could exist and it is believed that problems of a similar nature can be expected in other situations involving the application of dense porous plates such as the "Rigimesh" used in this facility. The screen section did an excellent job of reducing the level of vorticity in the chamber and forcing the streamwise velocity to be nearly constant across the chamber.

Screens may be the most practical and effective means of correcting mean velocity irregularities resulting from the dense porous plates. Comparing the spectra on both sides of the screens at given y/R locations (figures 11, 12, and 14-17) shows a reduction of the normalized turbulence intensities downstream of the screens for several different upstream disturbance levels. This occurred in spite of the fact that the mean velocities changed considerably across the screens at a given y/R location. It is believed that a second set of screens operating on the reduced turbulence levels and uniform flow distribution that resulted from the original set of seven screens in the tunnel (figures 24 and 25) would produce excellent

flow quality at the nozzle inlet. However, to obtain minimum disturbance levels it is well known that the mechanical quality of the screen installation must be excellent. Any minor damage to the screen mesh and any local slackness must be kept in repair which requires a design that allows convenient access to and removal of individual screens. Also the attachment of the screens to their support ring must be smooth and flush. The present installation was of poor quality in these areas, and with improvement in the mechanical design, the rather high turbulence levels, especially around the wall of the chamber, could probably be reduced.

This investigation was restricted by the fact that it was impossible to survey the flowfield at arbitrary streamwise or radial stations. Information could be obtained only at the four instrumentation ports shown on figure 1. If detailed progressive streamwise surveys would have been possible, they would have quantified the flow development associated with each turbulence manipulator as it related to the "entire chamber flow" and would have eliminated the need for speculation to interpret the results.

6. CONCLUDING REMARKS

The streamwise component of the mean and fluctuating velocities have been measured with a hot wire anemometer in the settling chamber of a blowdown supersonic pilot quiet tunnel. Distributions of these quantities across the chamber in the horizontal plane and simultaneous spectral analysis of the hot wire signal were obtained upstream and downstream of the 7 vorticity damping screens. Data were taken for various combinations of acoustic components consisting of a porous entrance diffuser cone, four porous plates, and a section filled with steel wool, all of which were installed upstream of the screens. Previous measurements of pressure fluctuations on the wall of the chamber showed that the porous components reduced the high level noise originating in the upstream pipes and control valves, by more than an order of magnitude in terms of the normalized rms pressures.

Comparisons of the pressure data with the hot wire data indicates that acoustic disturbances account for roughly one-half of the total rms velocity fluctuation levels of about 1 percent on the centerline downstream of the screens. Large increases in rms velocity fluctuations to about 10 percent off the centerline and the higher levels of about 15 percent upstream of the screens were due to vorticity generated directly by the porous plates or by the nonuniform mean velocity profiles downstream of the plates.

Tests made with the porous entrance cone, the downstream porous plate, or the steel wool removed, one at a time, showed

that both the mean and fluctuating flow was strongly affected by these components. For example, when the downstream porous plate was removed, the turbulence levels on the centerline downstream of the screens increased from about 1 to 1.5 percent but the distribution was much more uniform across the chamber. However, the cause of these flow changes could not be traced to any single component but rather to the combined effects of all components remaining in the chamber.

Downstream of the screens, the boundary layer thickness was about 15 percent of the chamber radius. The turbulence level generally increased to 3 or 4 percent outside the boundary layer. These high freestream levels were believed to be related to faulty techniques for attaching the porous plates and screens to their support liners.

The addition of a honeycomb or a high solidity perforated plate did not improve the flow quality. The honeycomb was probably too close to the upstream damping screen to allow sufficient distance for the flow disturbances caused by the honeycomb to decay. The perforated plate introduced high intensity discrete tones and probably also increased vorticity due to its high solidity.

The results indicate that improvements in the mechanical installation of the porous plates and damping screens and the use of porous plates with more uniform porosity should reduce the freestream velocity fluctuations to the minimum acoustic levels of about 0.5 percent.

REFERENCES

1. Anders, J. B., Stainback, P. C., Keefe, L. R., and Beckwith, I. E., "Fluctuating Disturbances in a Mach 5 Wind Tunnel", AIAA Journal, Vol. 15, No. 8, August 1977, pp. 1123-1129.
2. Laufer, J. and Marte, J. E., "Results and a Critical Discussion of Transition-Reynolds Numbers Measurements on Insulated Cones and Flat Plates in Supersonic Wind Tunnels", JPL Report No. 20-96, November 1955.
3. Laufer, J., "Aerodynamic Noise in Supersonic Wind Tunnels", Journal of the Aerospace Sciences, Vol. 28, No. 9, September 1961, pp. 685-692.
4. Laufer, J., "Factors Affecting Transition Reynolds Numbers on Models in Supersonic Wind Tunnels", Journal of Aeronautical Sciences, Vol. 21, No. 7, July 1954, pp. 497-498.
5. Mabey, D. J., and Sawyer, W. G., "Reduction of Flow Unsteadiness in the 3 ft x 4 ft Supersonic Tunnel", Royal Aircraft Establishment, Technical Report 73194, December 1973.
6. Jones, R. A., and Feller, W. V., "Preliminary Surveys of the Wall Boundary Layer in a Mach 6 Axisymmetric Tunnel", NASA Technical Note D-5620, February 1970.
7. Amick, J. L., "Design and Performance of the University of Michigan 6.6-Inch Hypersonic Wind Tunnel", NASA Contractor Report 2569, July 1975.
8. Lau, Y. L., and Baines, W. D., "Flow of Stratified Fluid

- Through Curved Screens", Journal of Fluid Mechanics, Vol. 33, Part 4, 1968, pp. 721-738.
9. Nagib, H. M., and Loehrke, R. I., "Experiments on Management of Free-Stream Turbulence", AGARD Report No. 598, September 1972.
 10. Wigeland, R. A., Tan-atichat, J., and Nagib, H. M., "Evaluation of a New Concept for Reducing Free-Stream Turbulence in Wind Tunnels", NASA Contractor Report 3196, October 1979.
 11. Way, J. L., Nagib, H. M., and Tan-atichat, J., "On Aero-Acoustic Coupling in Free-Stream Turbulence Manipulators", AIAA Aero-Acoustics Conference, Seattle, Washington, October 15-17, 1973.
 12. Bonnet, J. P., and Roquefort, T. A., "Determination and Optimization of Frequency Response of Constant Temperature Hot-Wire Anemometers in Supersonic Flow", Review of Scientific Instrumentation, Vol. 51, No. 2, February 1980.
 13. Beckwith, I. E.: Comments on Settling Chamber Design for Quiet, Blowdown Wind Tunnels. NASA TM-81948, March 1981.
 14. Anders, J. B., Stainback, P. C., Keefe, L. R., and Beckwith, I. E., "Sound and Fluctuating Disturbance Measurements in the Settling Chamber and Test Section of a Small, Mach 5 Wind Tunnel", Sixth International Congress on Instrumentation in Aerospace Simulation Facilities, Ottawa, Canada, September 22-24, 1975.





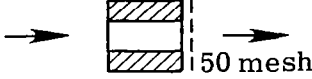
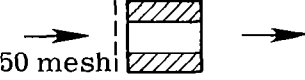
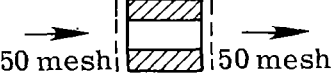
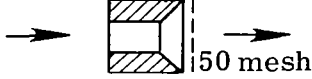
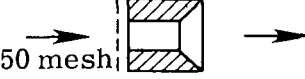
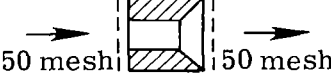



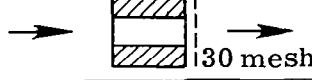
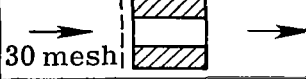
#	Description	Velocity (m/sec)		
		30.5	61.0	122.0
1.		79.5 dB	82 dB	87 dB
2.		80.5	86	88
3.		82	86	87
4.		84	87	87
5.		78	80	80
6.		78	80	82.5
7.		77	79	79.5
8.		80	84.5	88
9.		79	82	84
10.		79	83	86
11.		80	82.5	83.5
12.		81	85	87
13.		81	84	85
14.		77	80	80.5
15.		78	80	82.5

Table 1.- Sound intensities measured in decibels resulting from flow through various orifice plates, background noise is 66 dB.

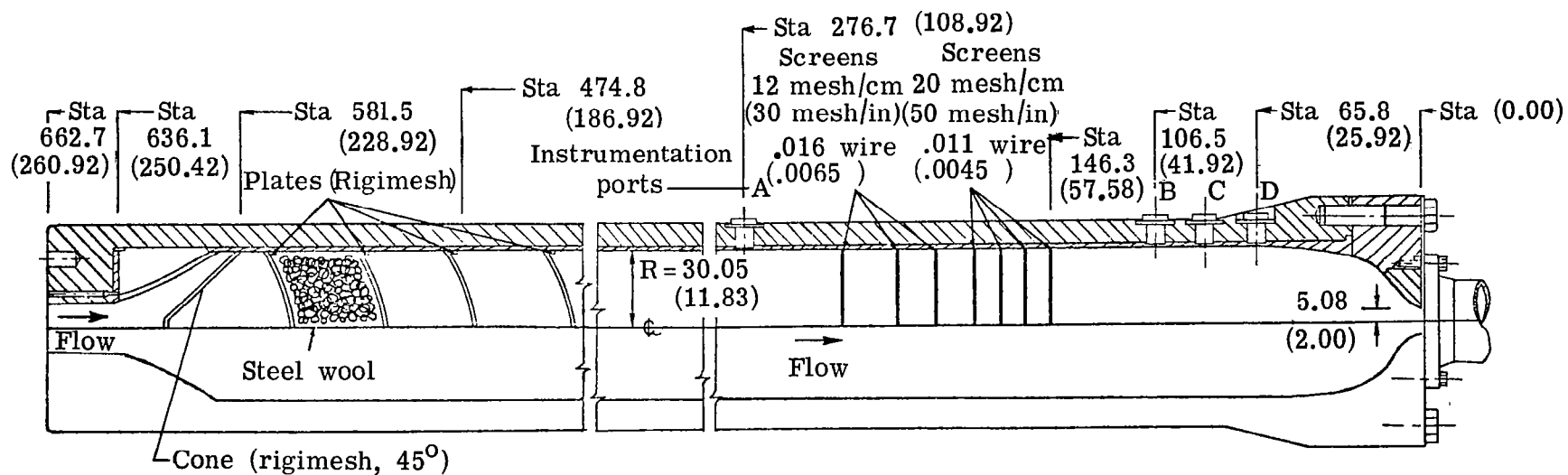


Figure 1.- Plan view of original complete settling chamber for the Supersonic Pilot Quiet Tunnel. Porous ("Rigimesh") plates and cone are 0.64 cm (0.25 in.) thick. All dimensions and stations in cm (inches).

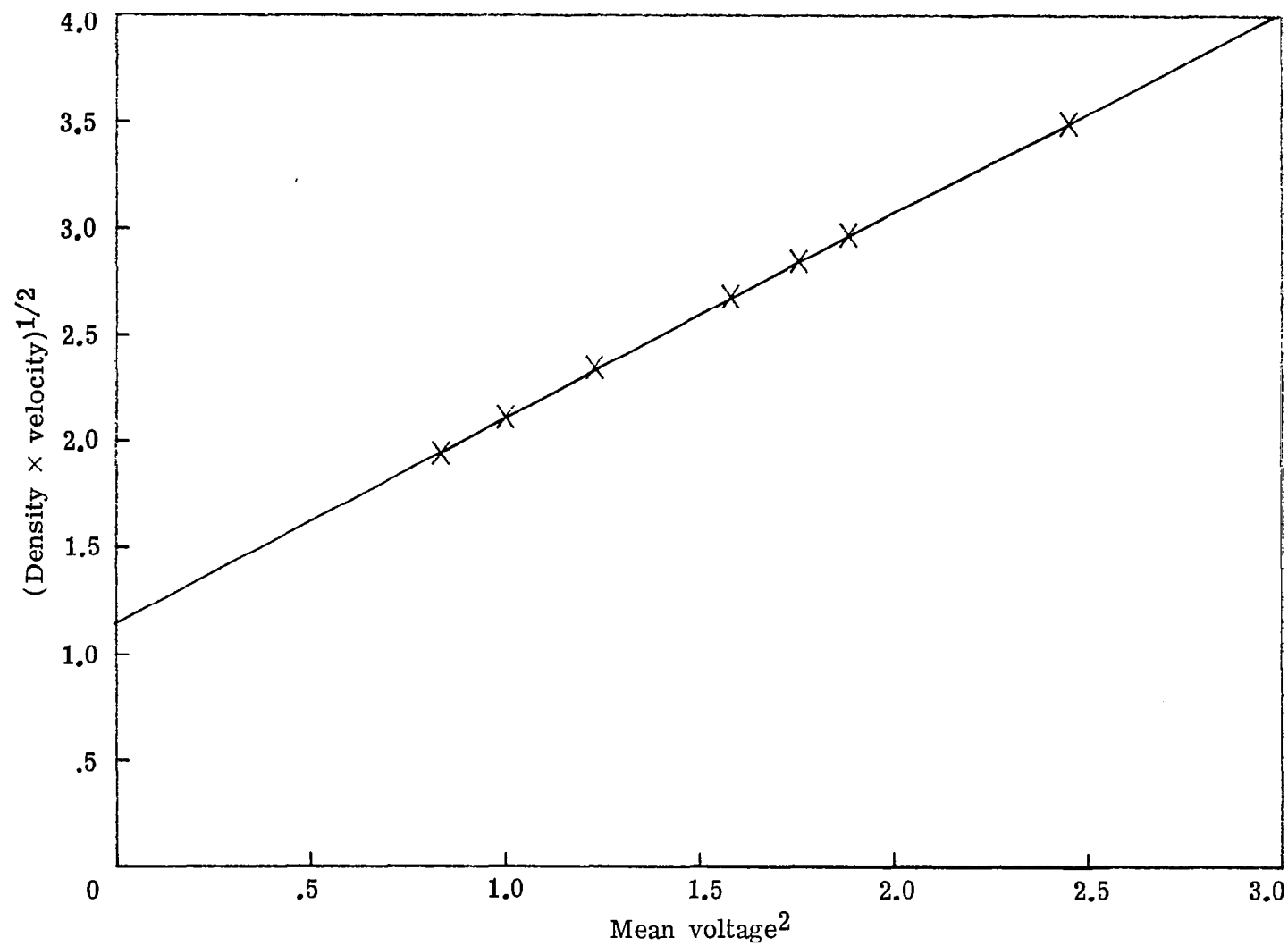


Figure 2.- Hot-wire calibration. (Wire dia. = $2.54\mu\text{m}$, material = pt/10%Rh)

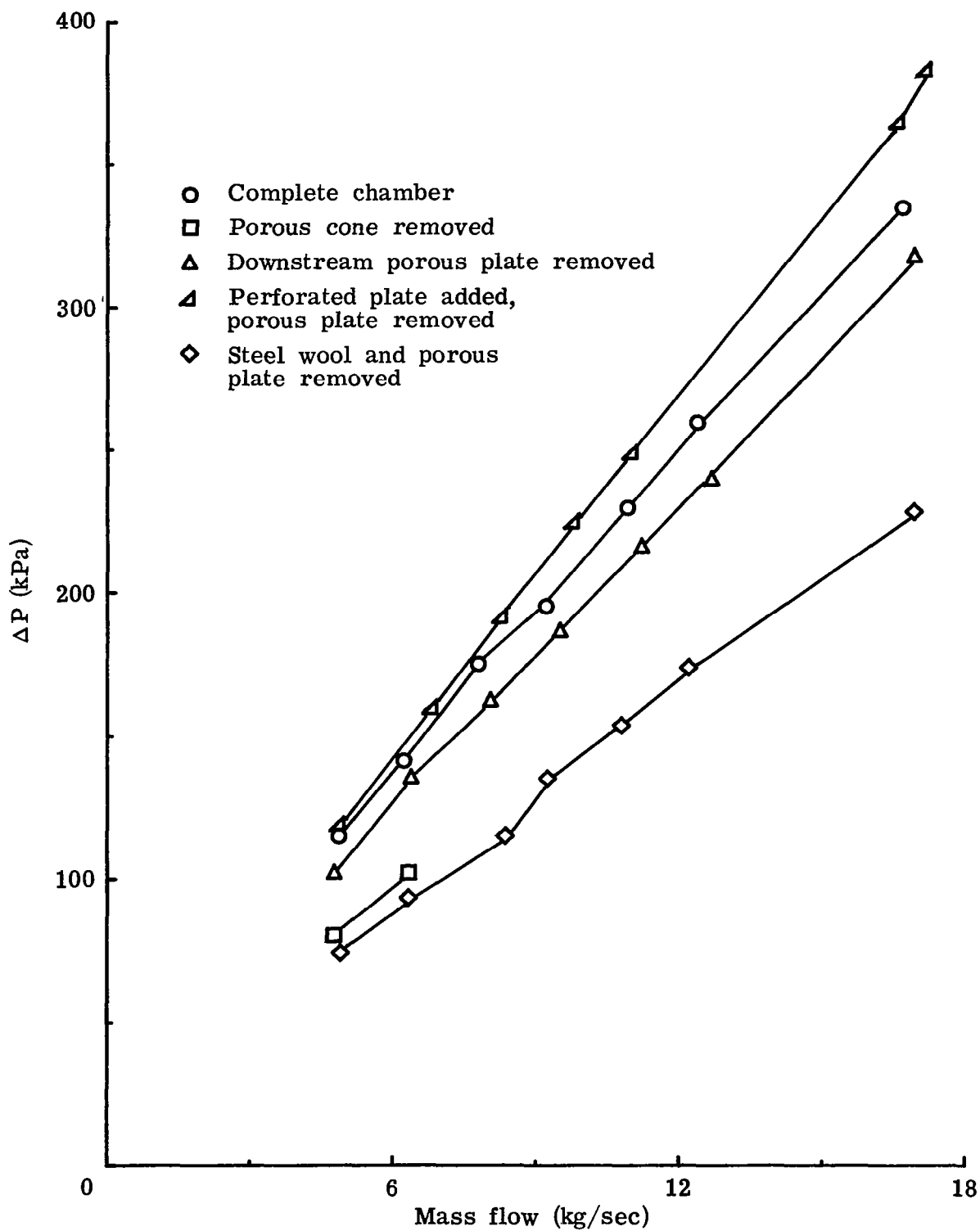


Figure 3.- Total pressure drop across the settling chamber for several configurations.

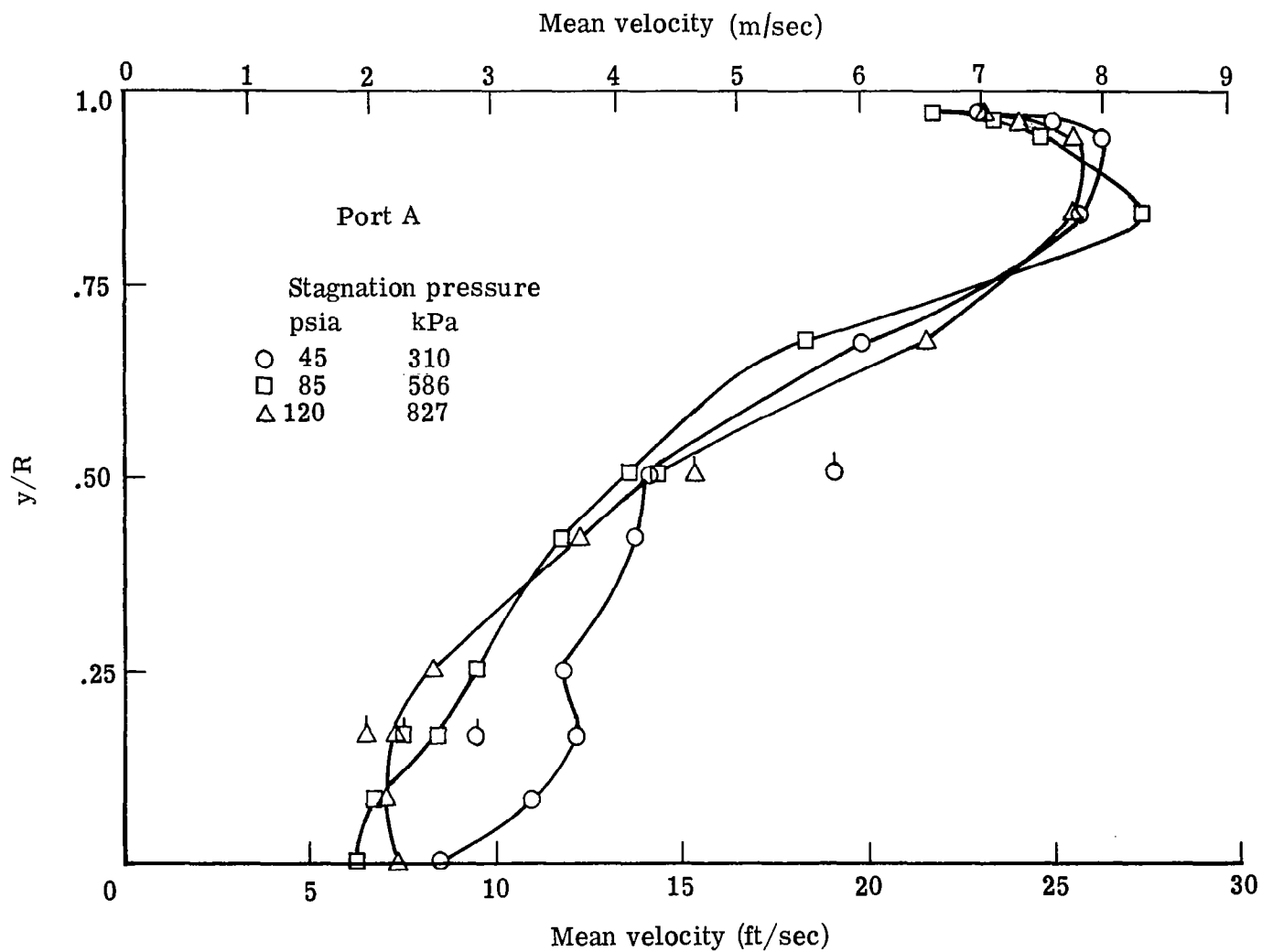


Figure 4.- Mean velocity profiles at Port A in the complete chamber.

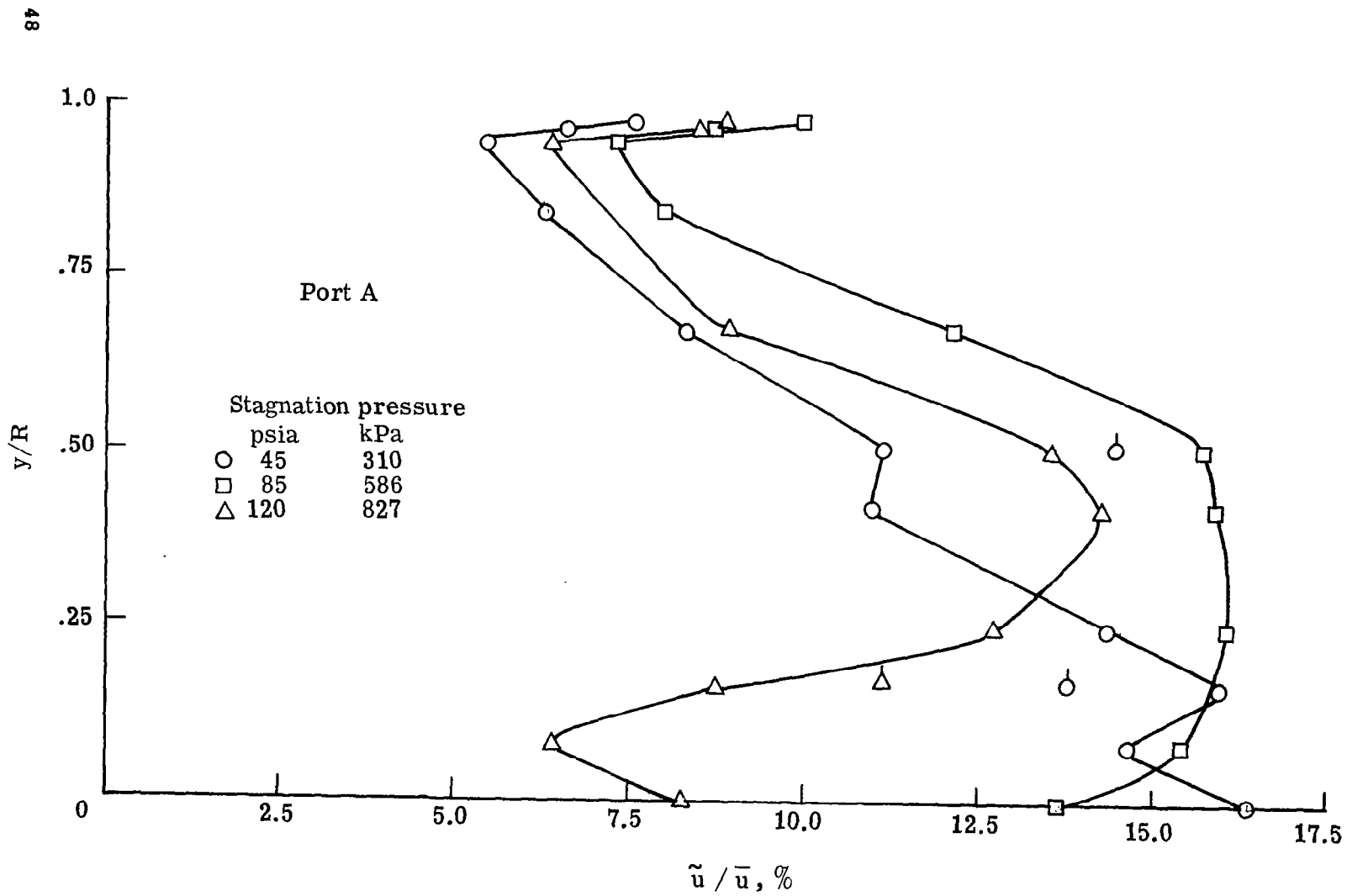


Figure 5.- Fluctuating velocity distributions at Port A in the complete chamber.

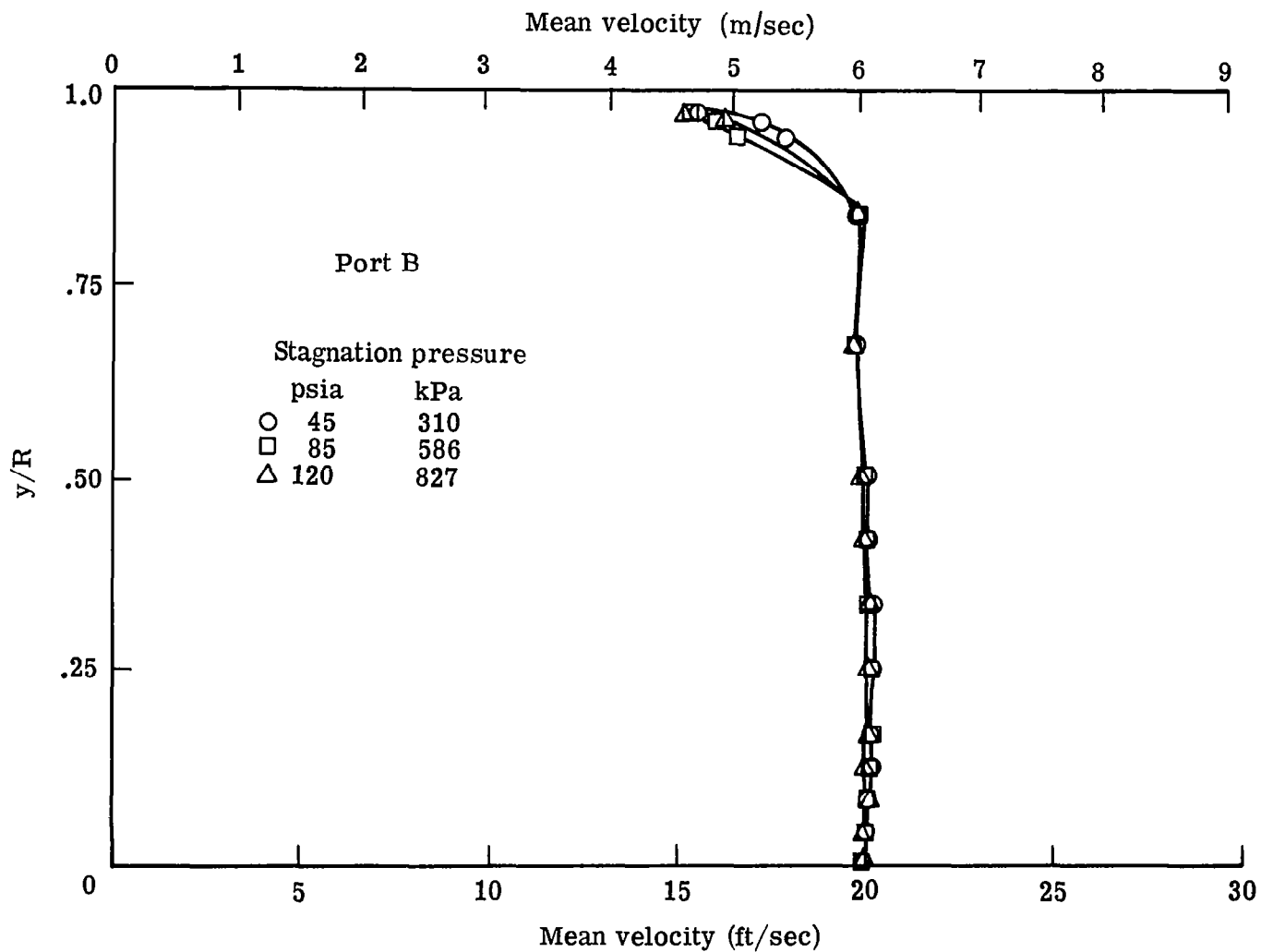


Figure 6.- Mean velocity profiles at Port B in the complete chamber.

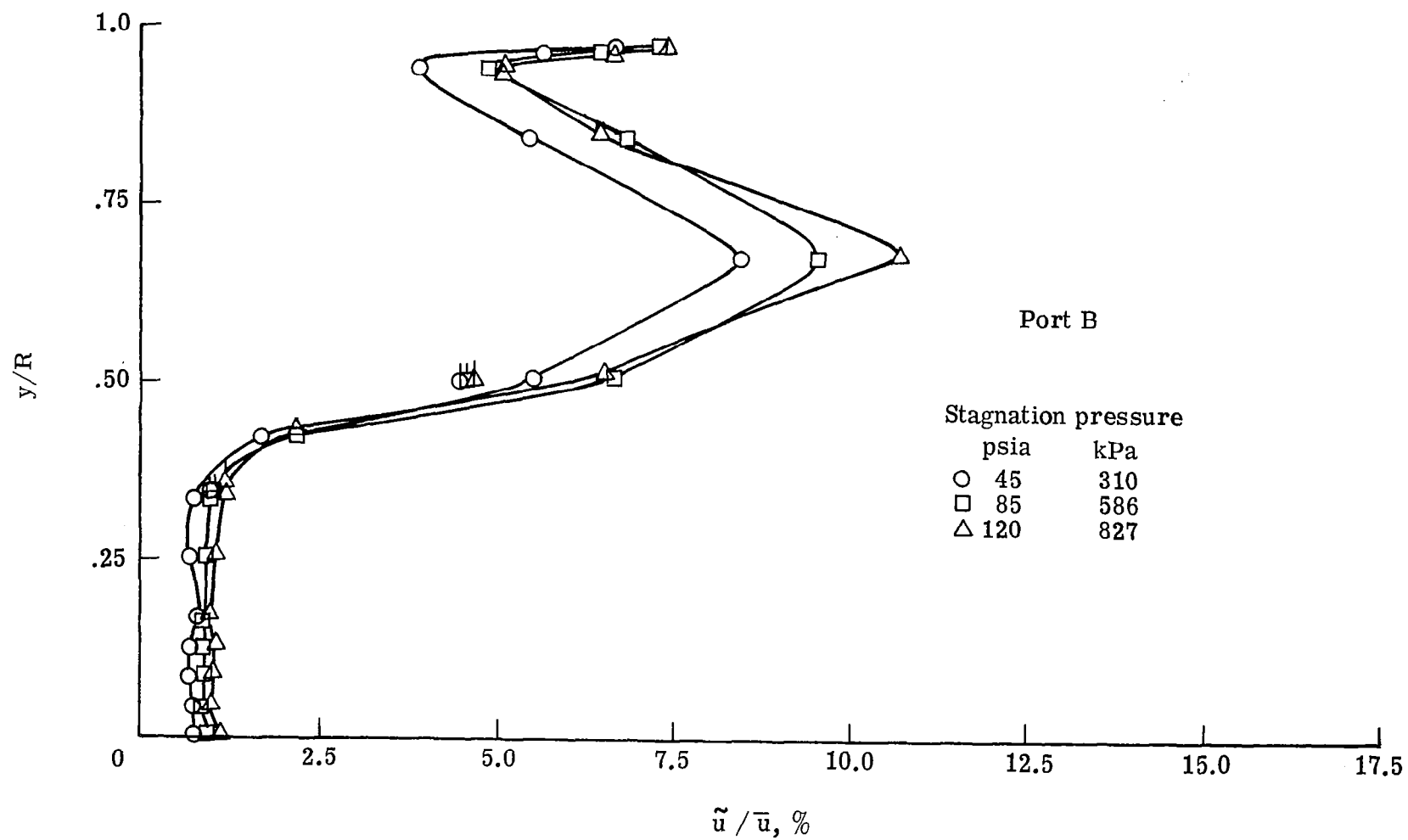


Figure 7.- Fluctuating velocity distributions at Port B in the complete chamber.

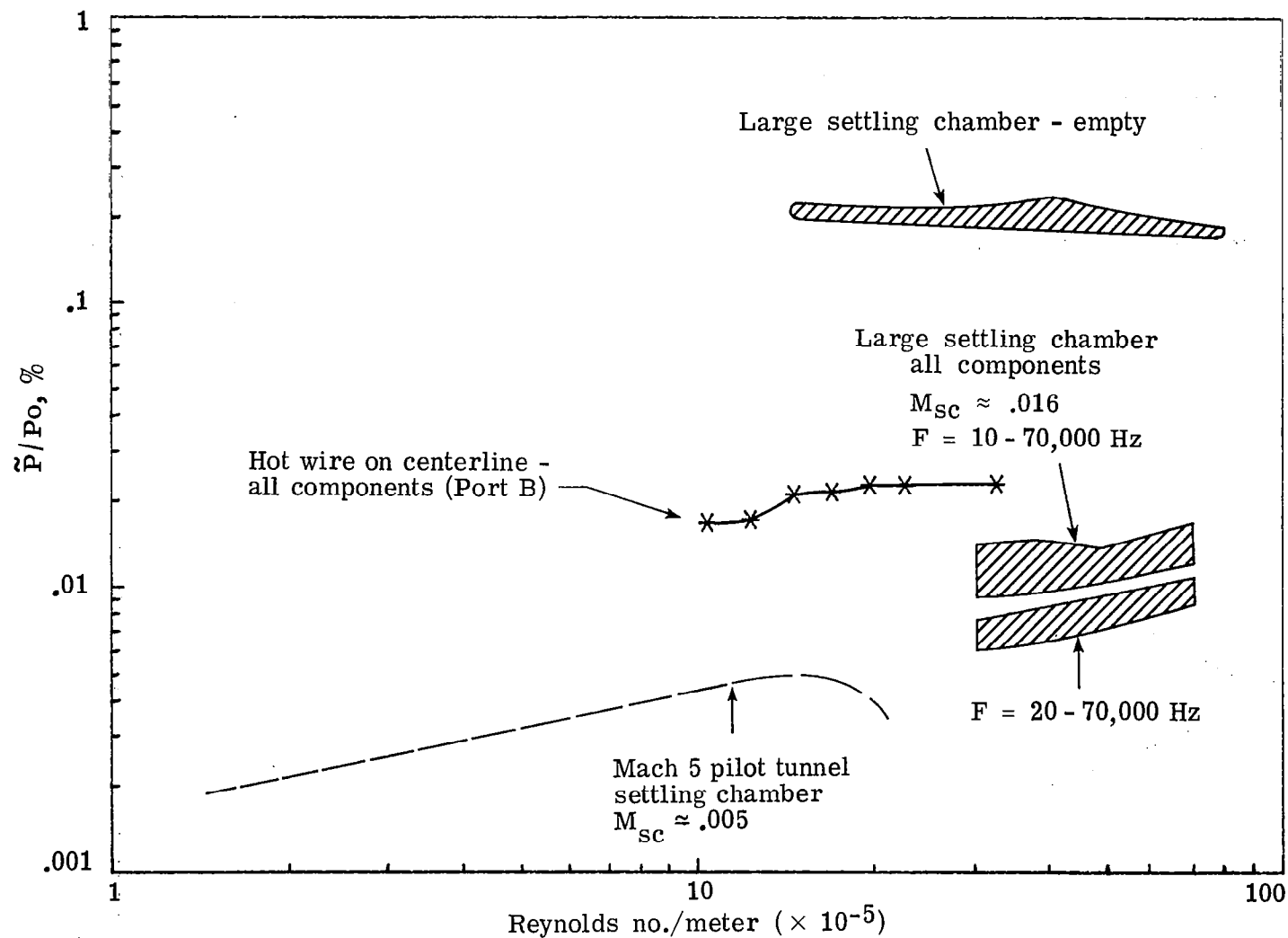


Figure 8.- Acoustic pressure fluctuations in the settling chamber at Port D.
 Pressure transducer data obtained by J. Wayne Keys, NASA Langley.

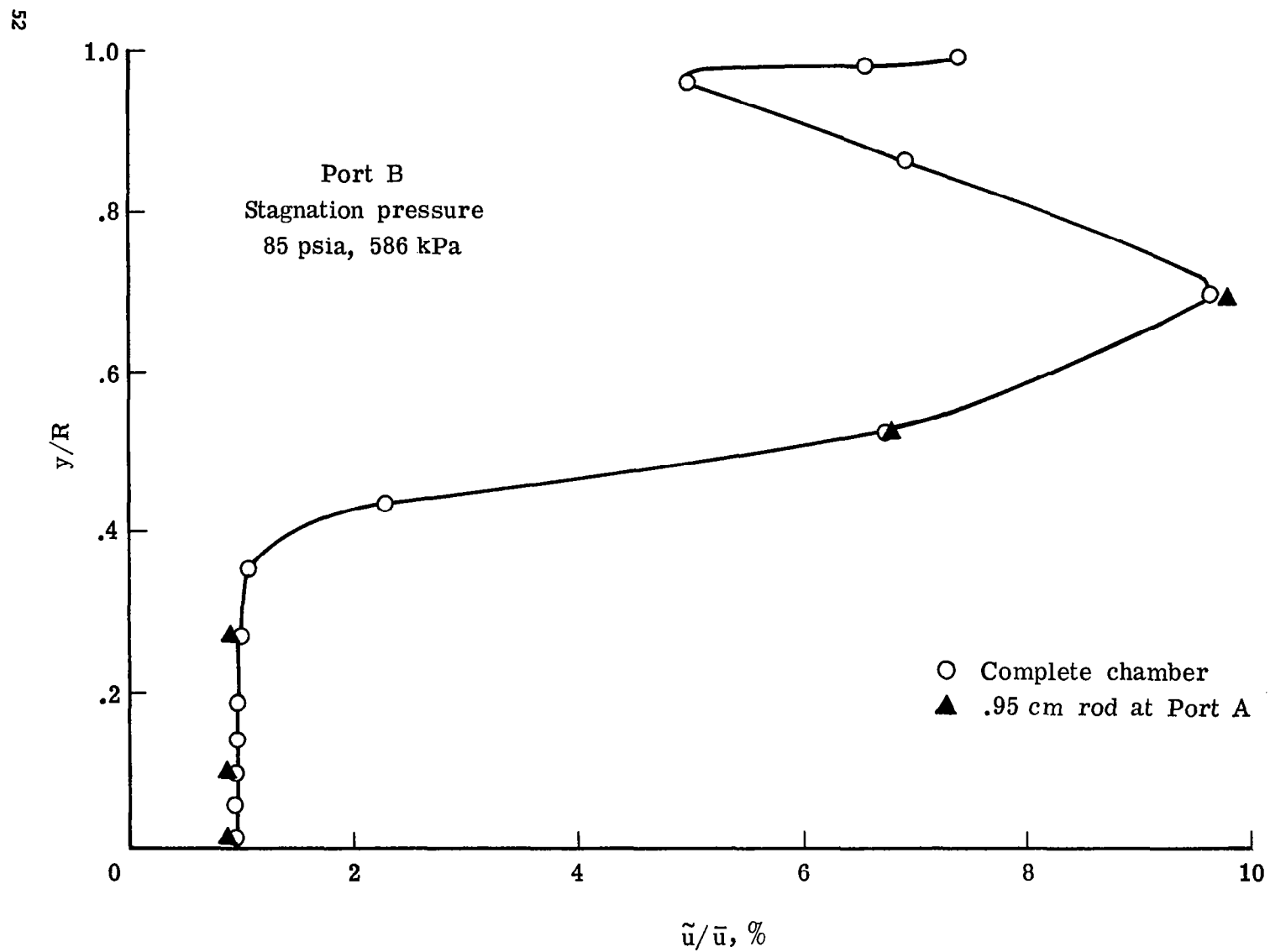


Figure 9.- Effects of rod at upstream location on velocity fluctuation distribution at Port B.

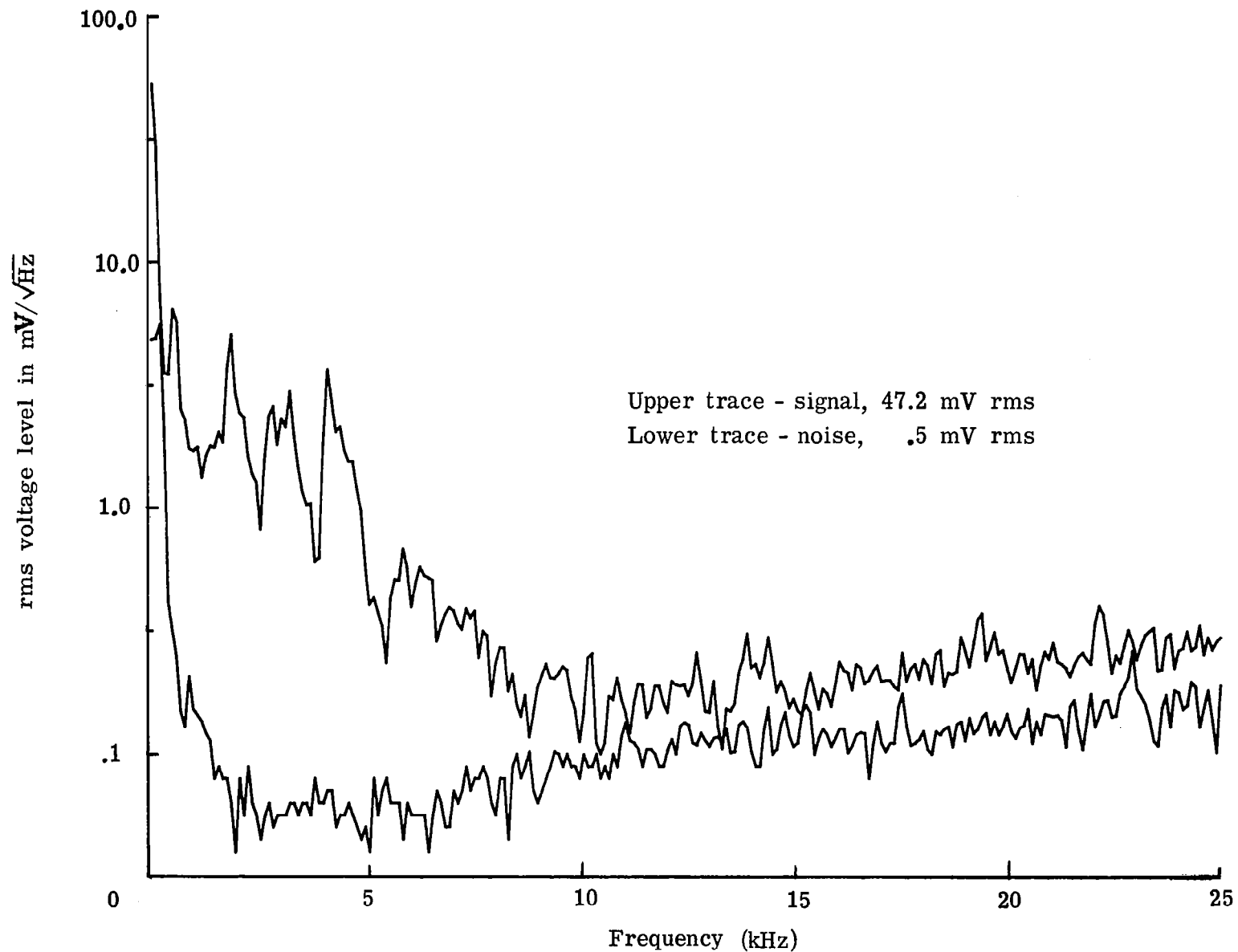


Figure 10.- Comparison of hot wire signal and electronic noise spectra at Port B with all components installed. $y/R = 0.67$, $P_o = 586 \text{ kPa}$ (85 psia).

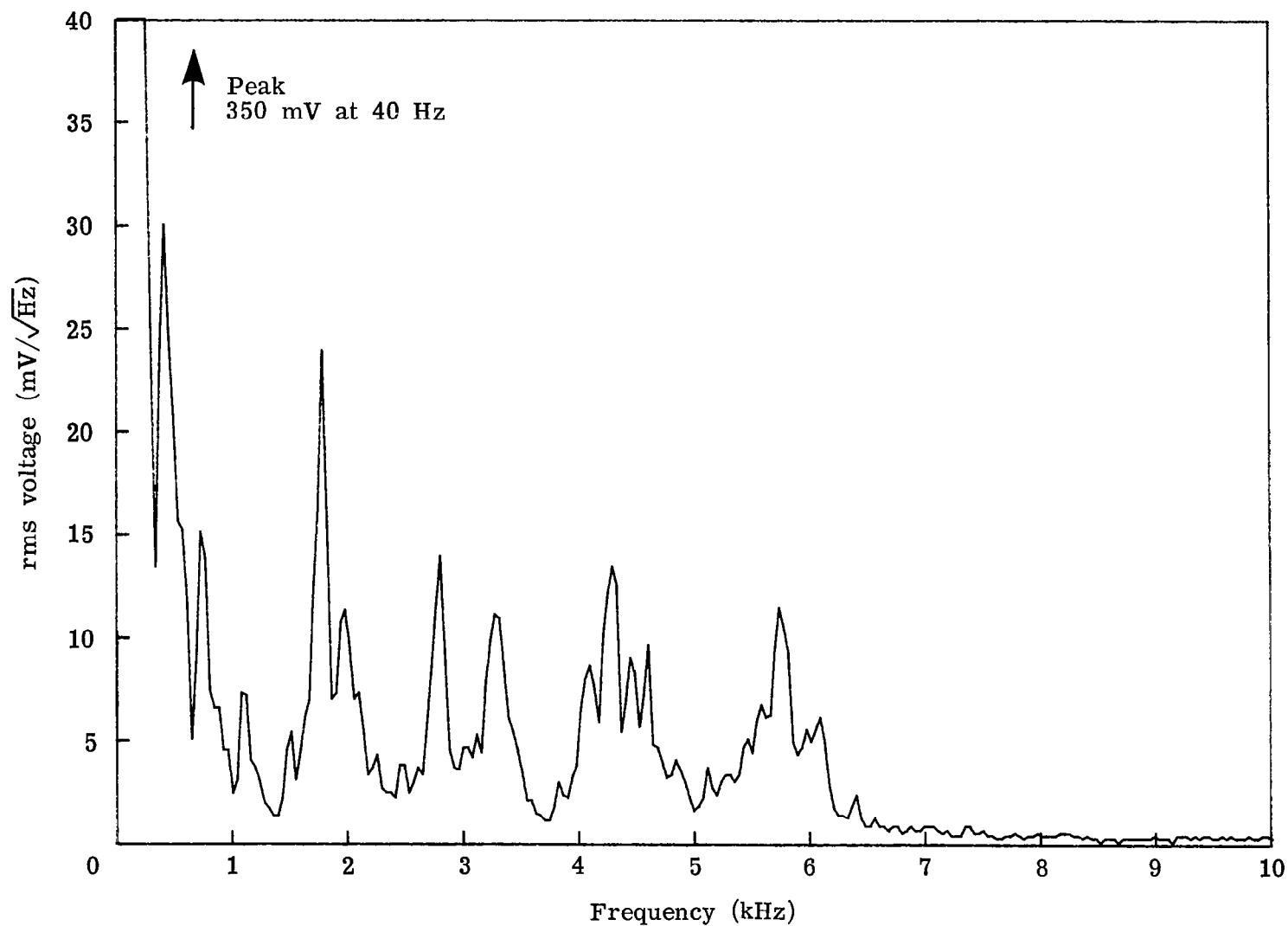
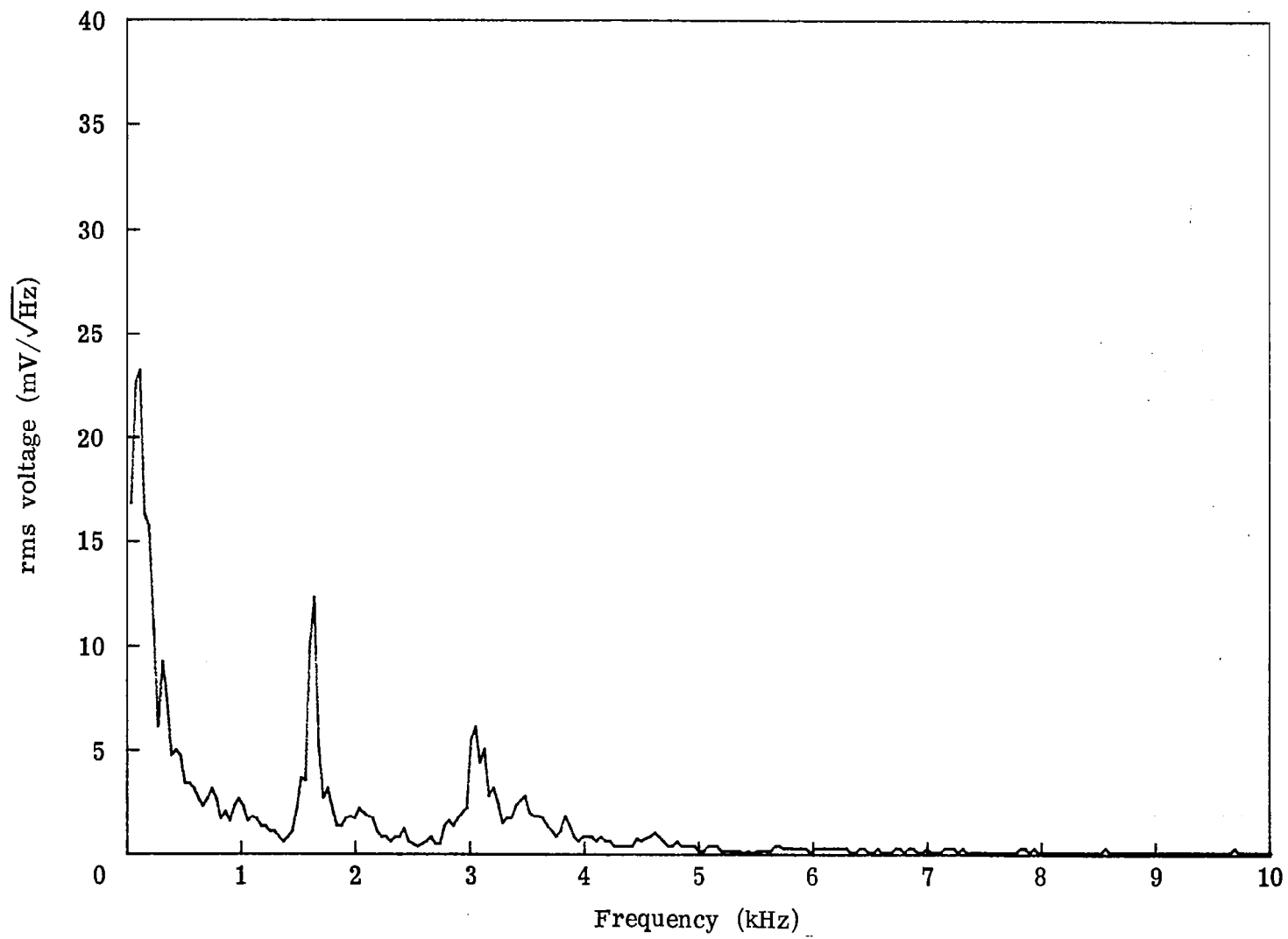


Figure 11.- Hot-wire spectra in complete chamber. Reynolds no./meter = 2.25×10^6 ,
Port A, $y/R = 0$.



55 Figure 12.- Hot wire spectra in complete chamber. Reynolds no./meter = 2.25×10^6 ,
Port B, $y/R = 0$.

Upper trace ($y/R = 0$) Lower trace ($y/R = .67$)

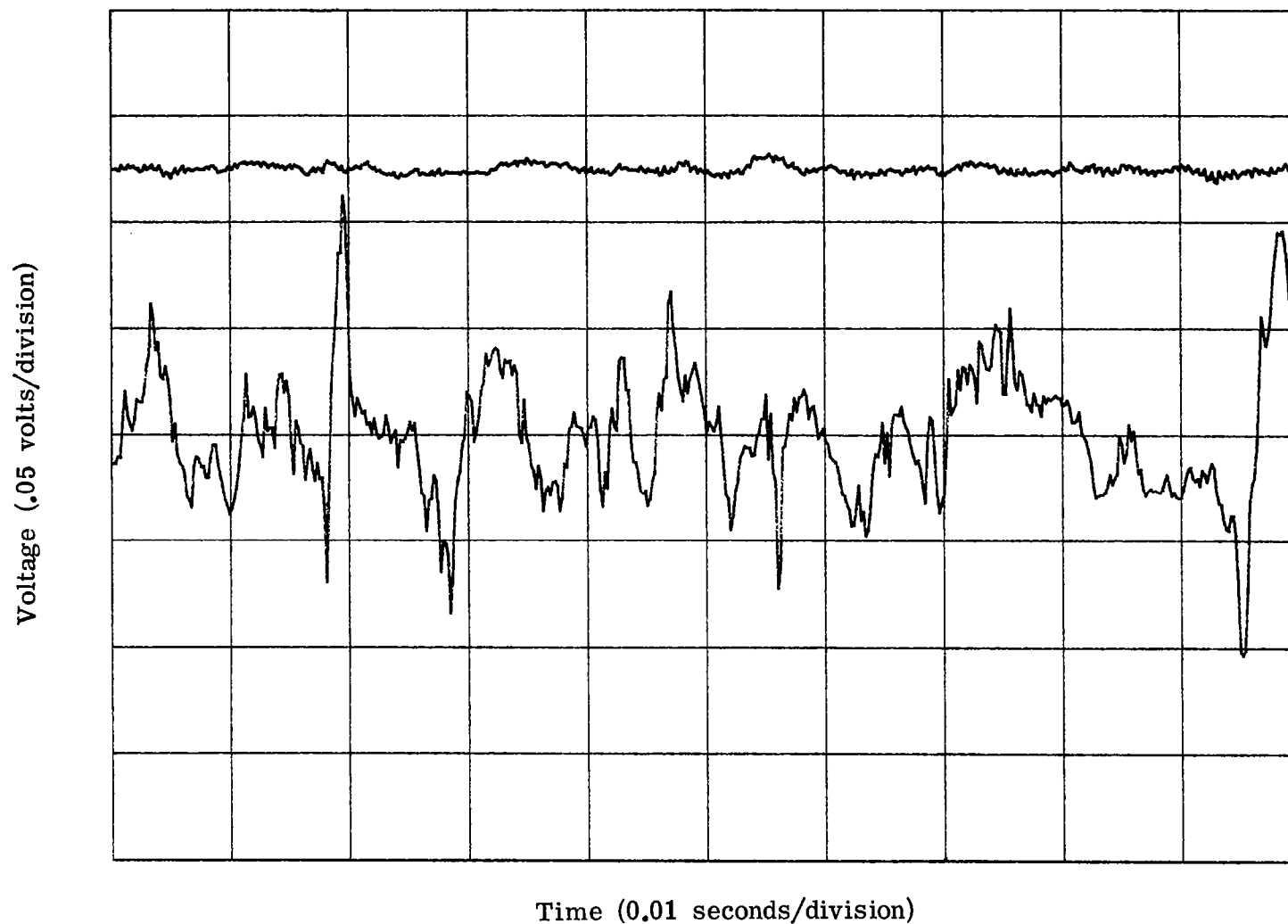


Figure 13.- Comparison of time signals on and off the centerline at Port B.
Reynolds no./meter = 2.25×10^6 .

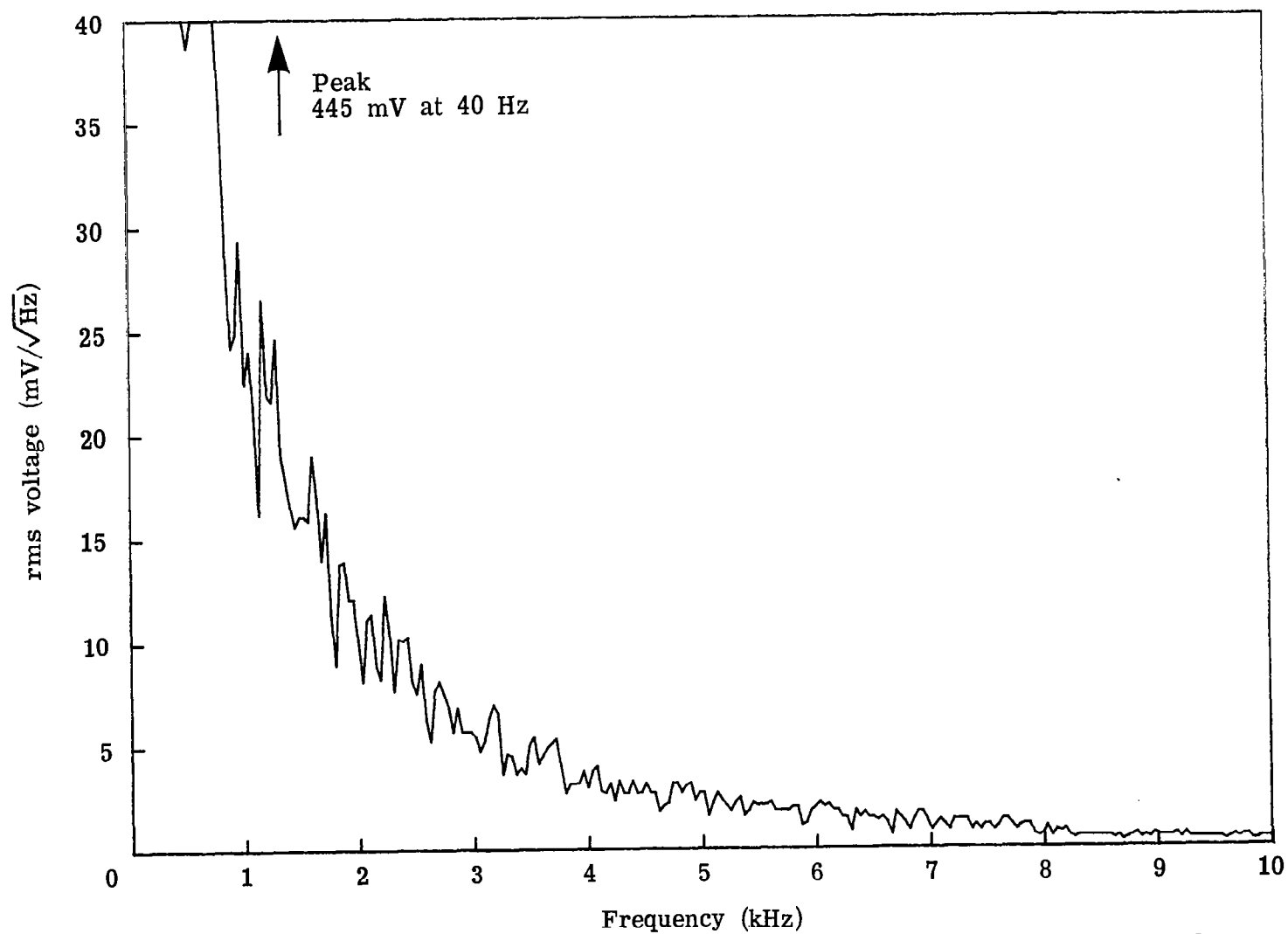


Figure 14.- Hot-wire spectra in complete chamber. Reynolds no./meter = 2.25×10^6 ,
Port A, $y/R = .67$.

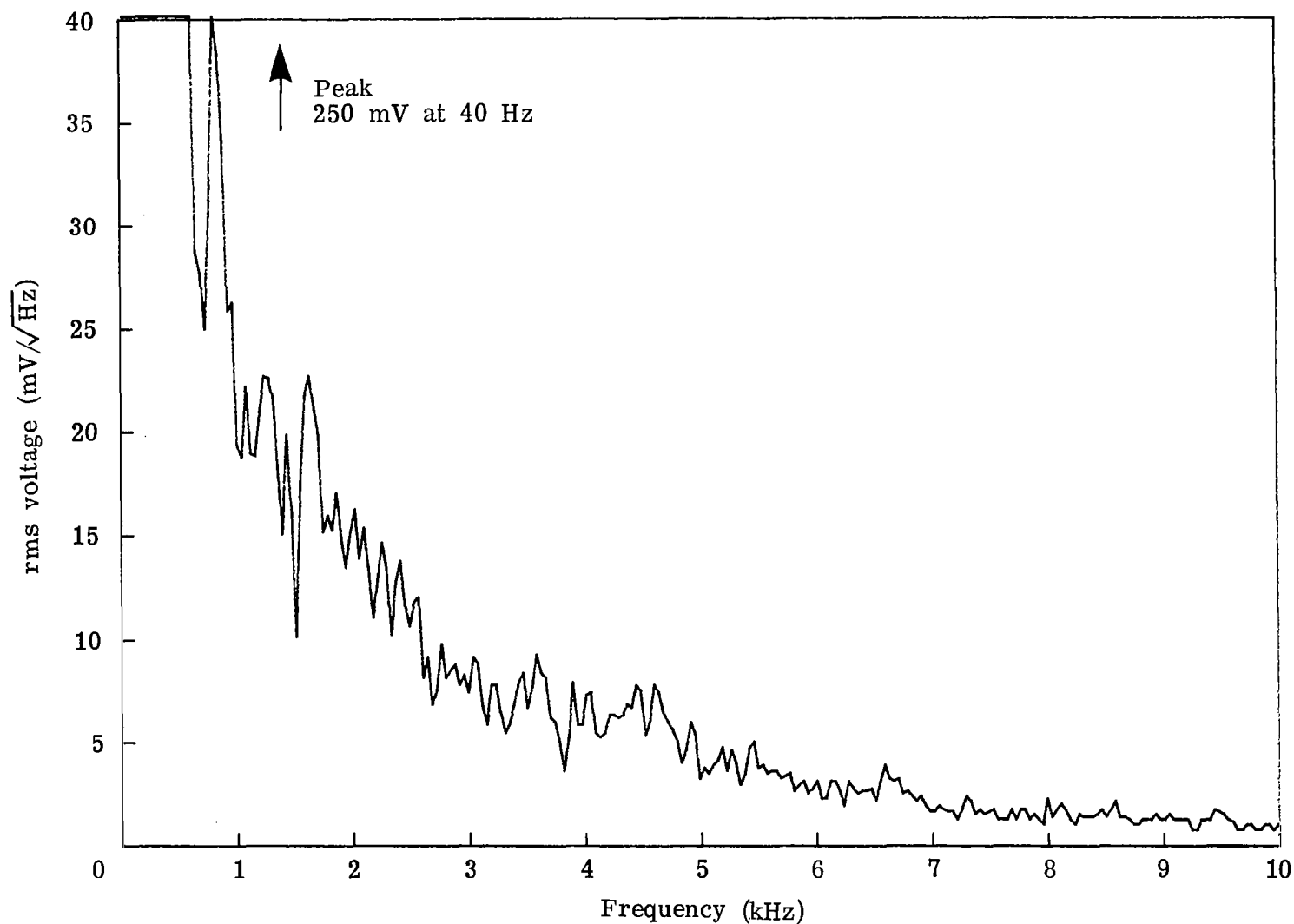


Figure 15.- Hot-wire spectra in complete chamber. Reynolds no./meter = 2.25×10^6 ,
Port B, $y/R = .67$.

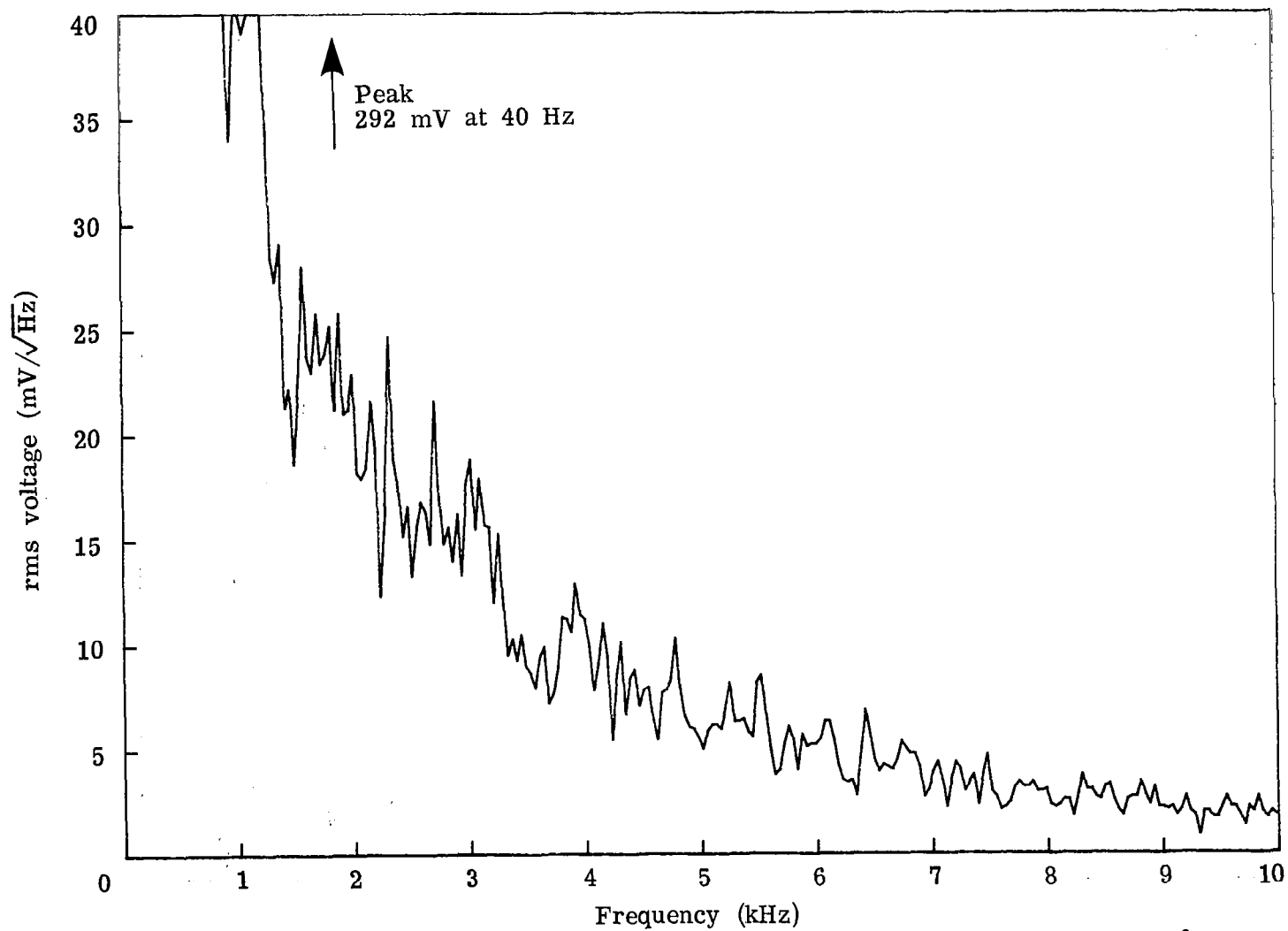


Figure 16.- Hot-wire spectra in complete chamber. Reynolds no./meter 2.25×10^6 ,
Port A, $y/R = .975$.

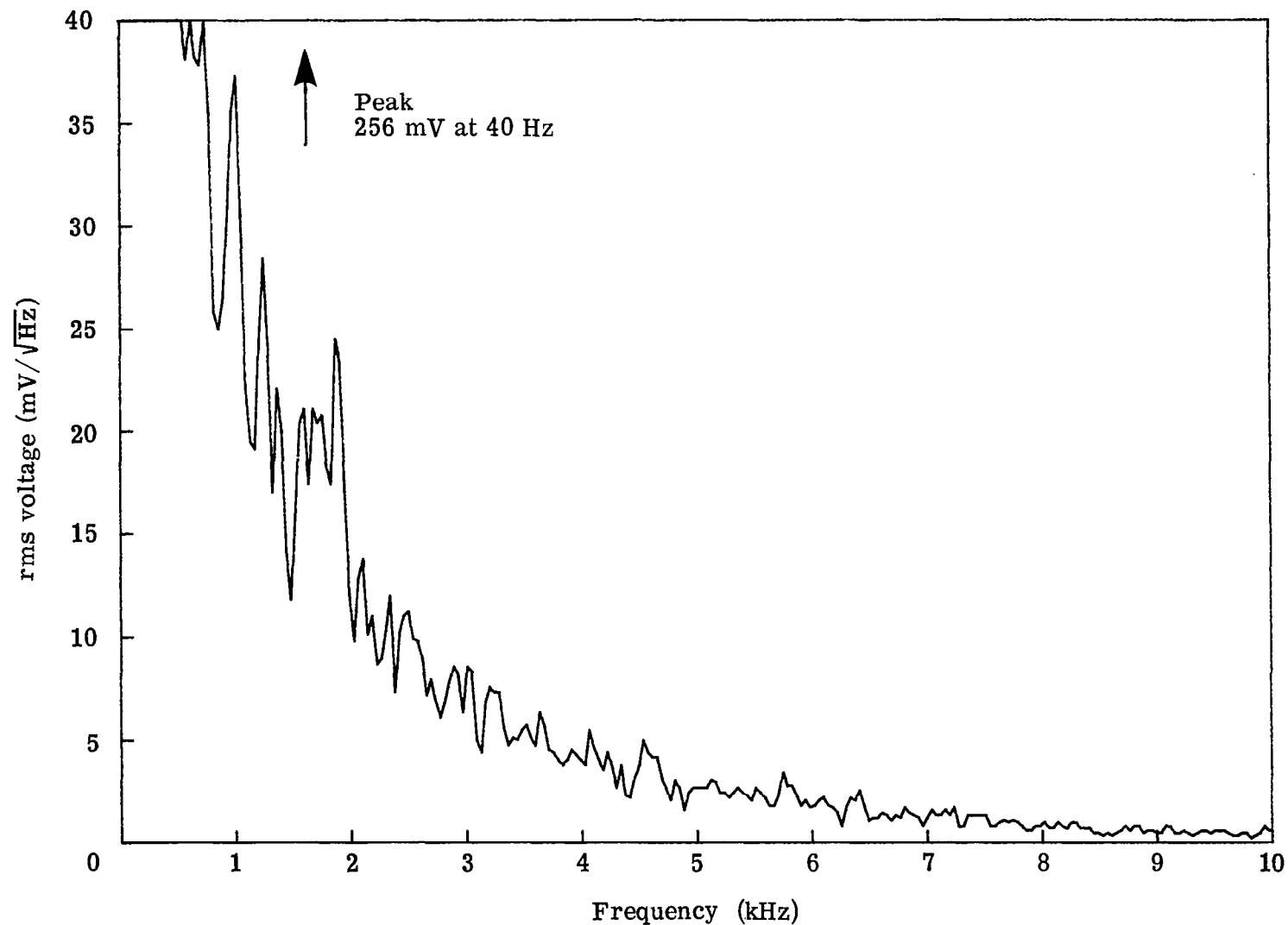


Figure 17.- Hot-wire spectra in complete chamber. Reynolds no./meter 2.25×10^6 ,
Port B, $y/R = .975$

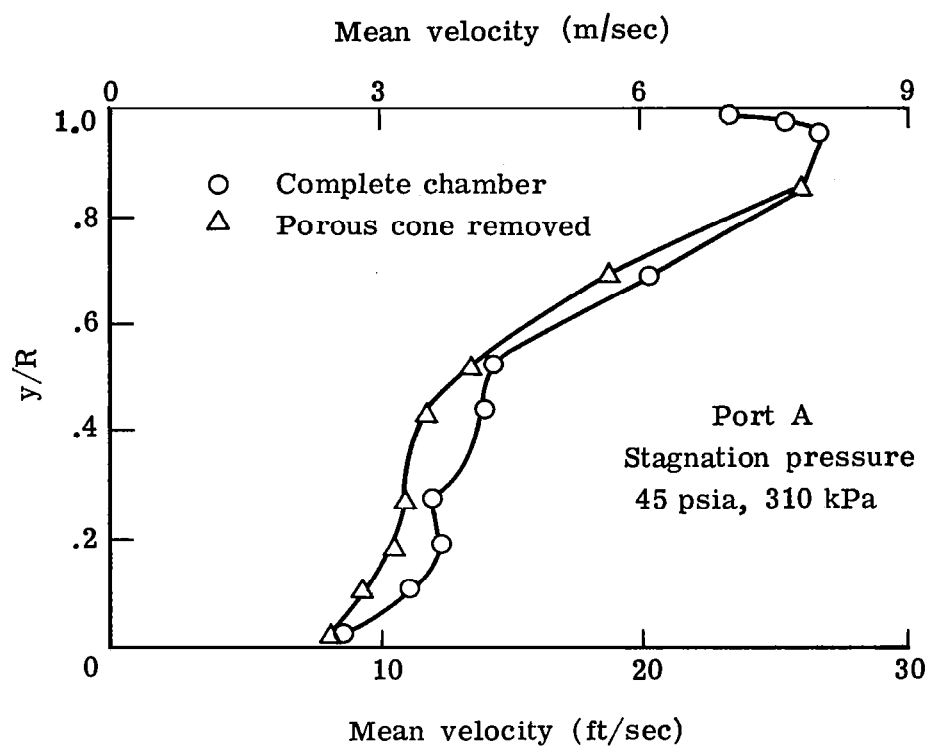


Figure 18.- Mean velocity profiles at port A with and without porous cone.

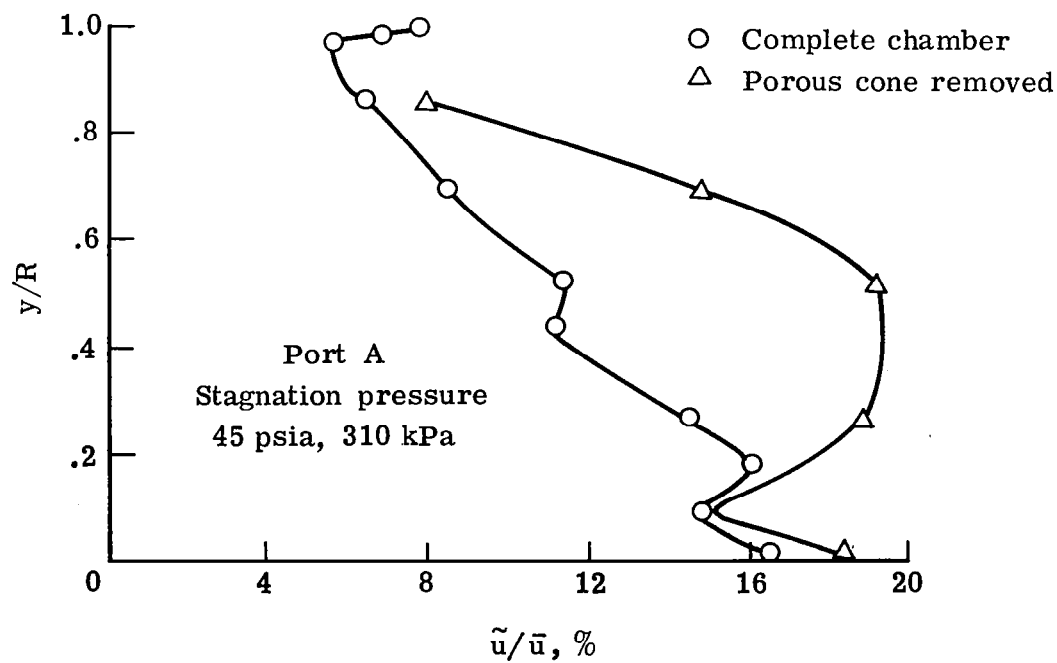


Figure 19.- Rms velocity fluctuations at Port A with and without porous cone.

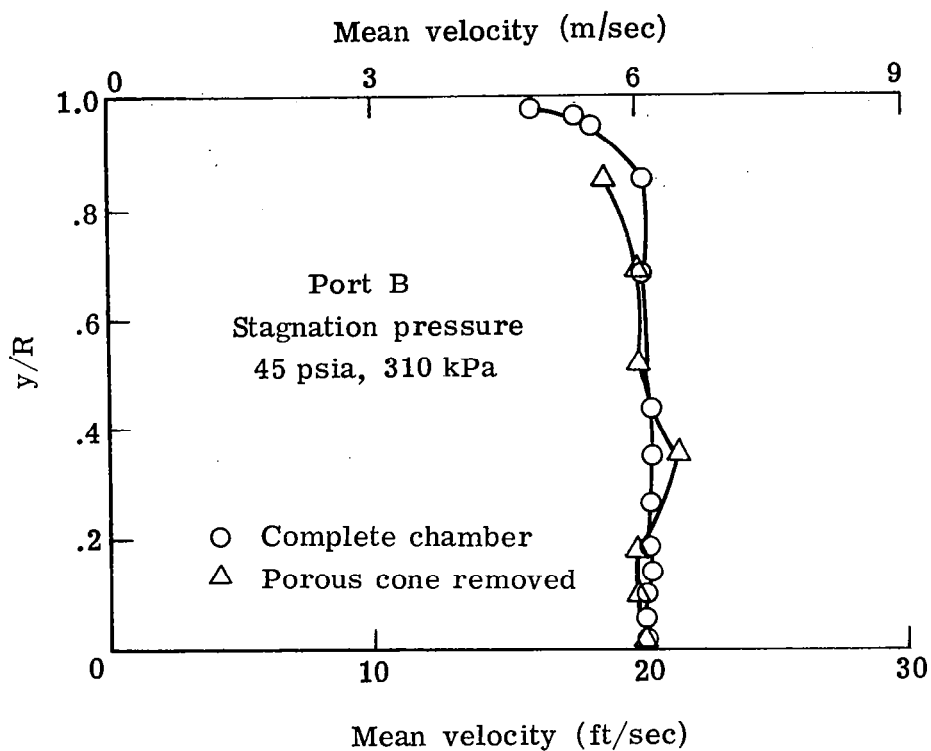


Figure 20.- Mean velocity profiles at port B with and without porous cone.

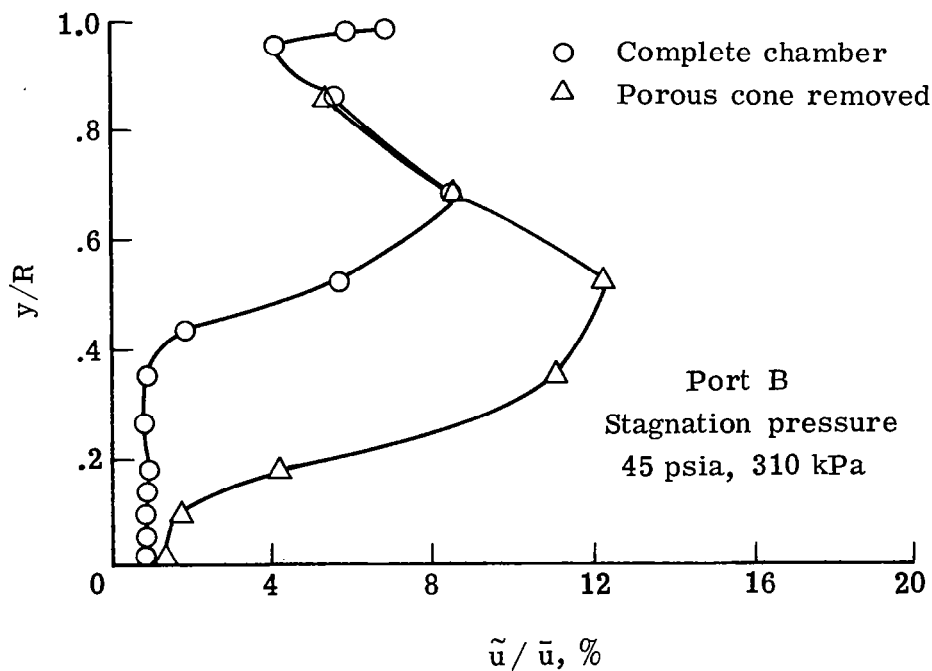


Figure 21.- Rms velocity fluctuations at Port B with and without porous cone.

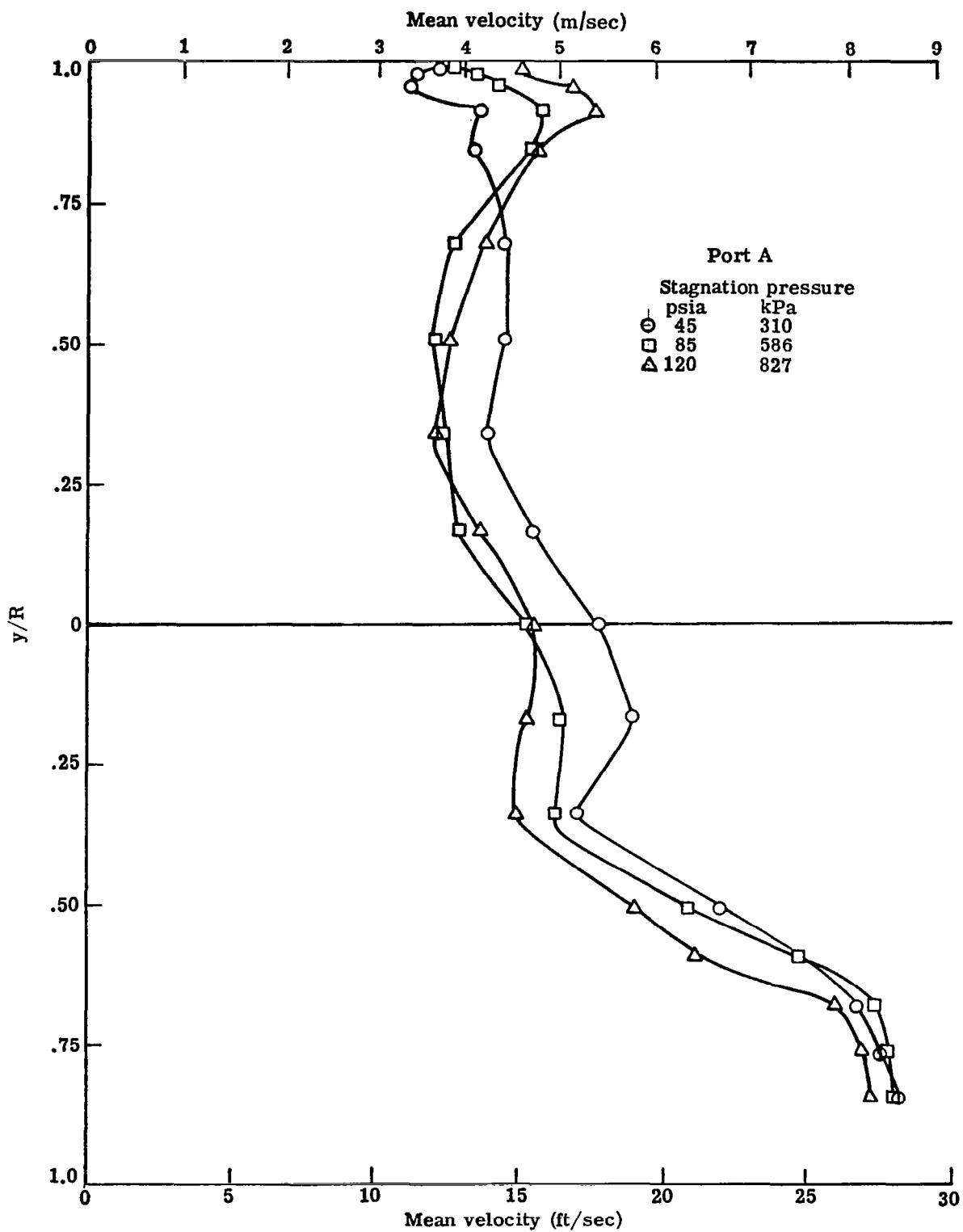


Figure 22.- Mean velocity profiles at Port A with downstream porous plate removed from the chamber.

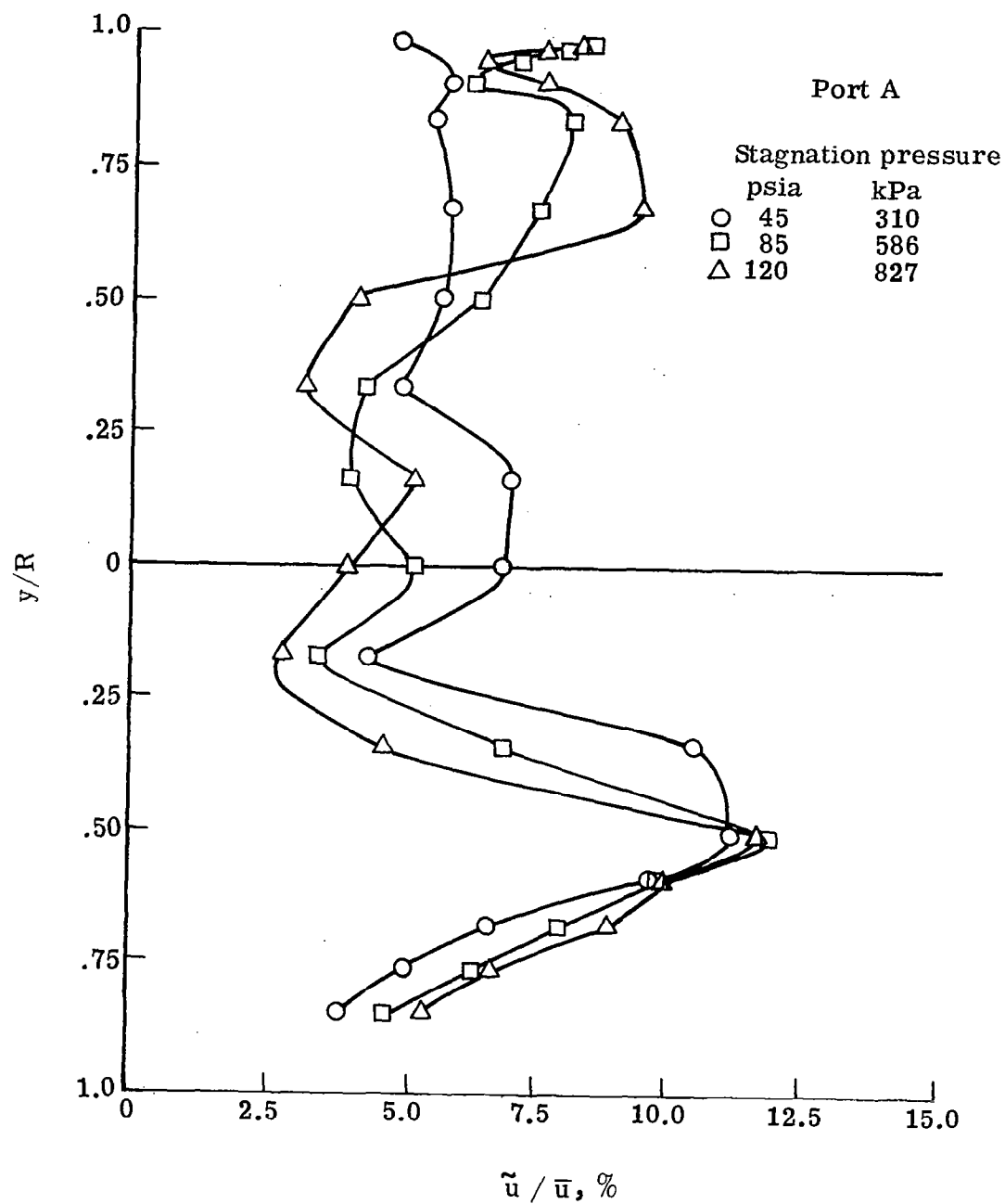


Figure 23.- Fluctuating velocity distributions at Port A with downstream porous plate removed from the chamber.

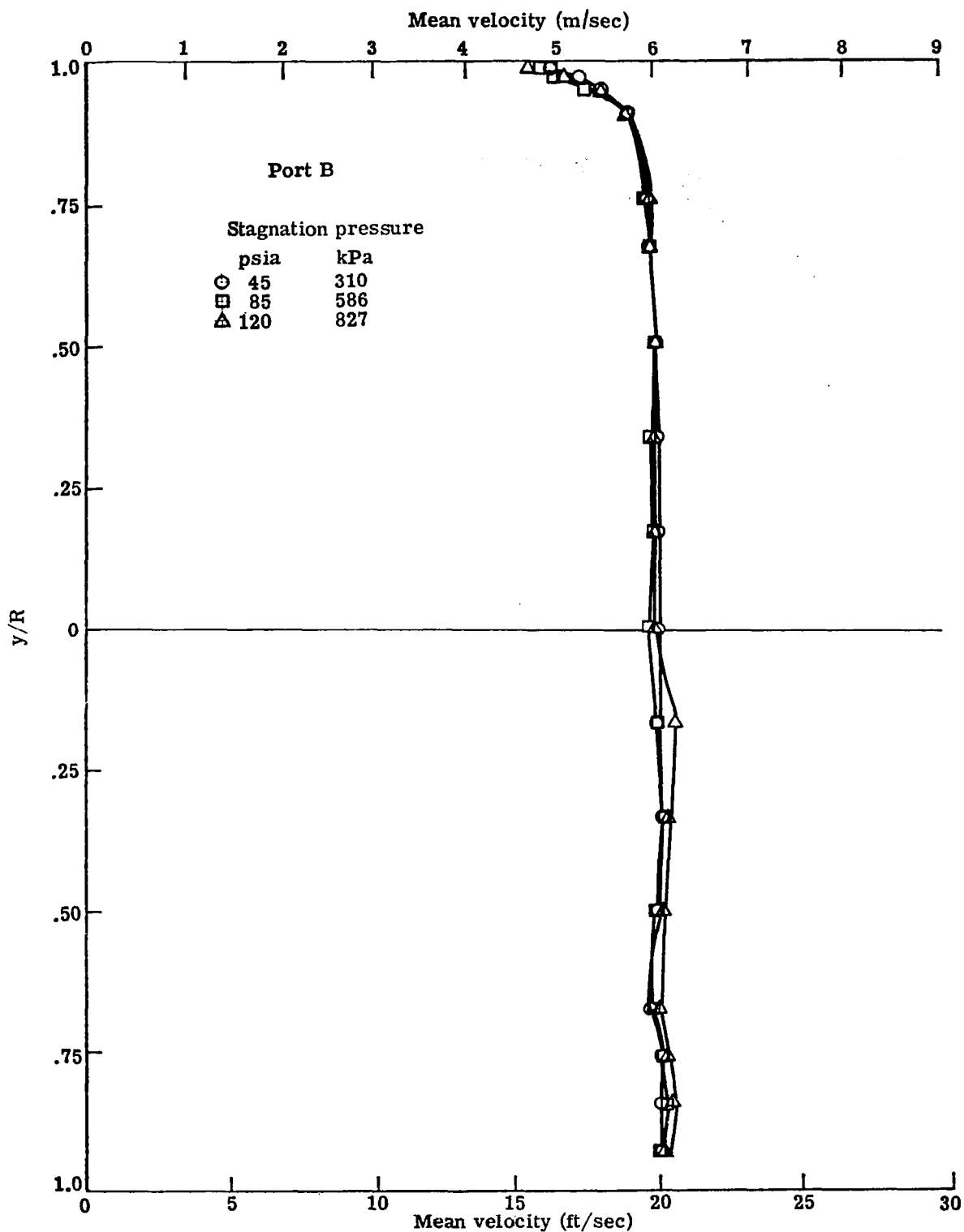


Figure 24.- Mean velocity profiles at Port B with downstream porous plate removed from the chamber.

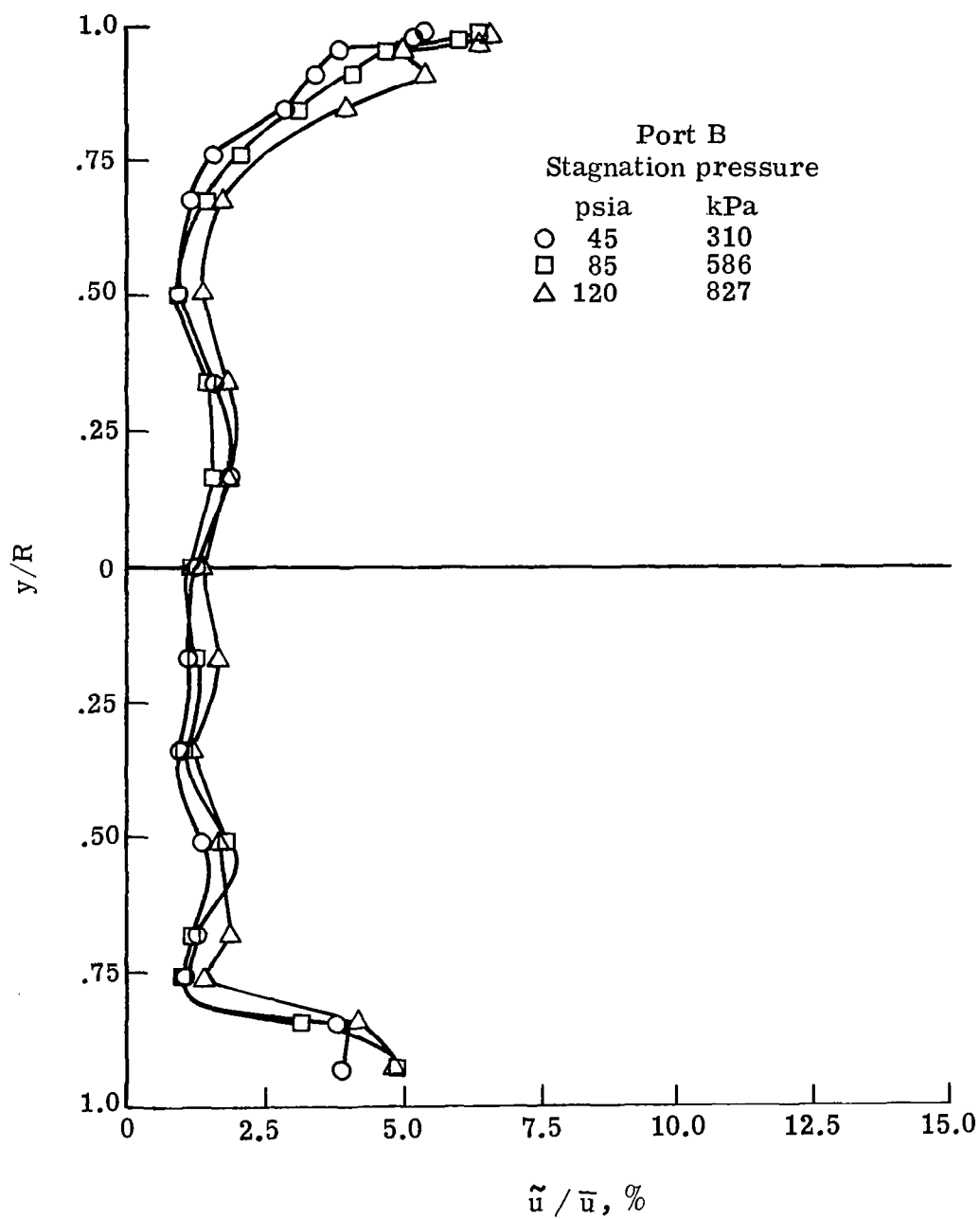


Figure 25.- Fluctuating velocity distributions at Port B with downstream porous plate removed from the chamber.

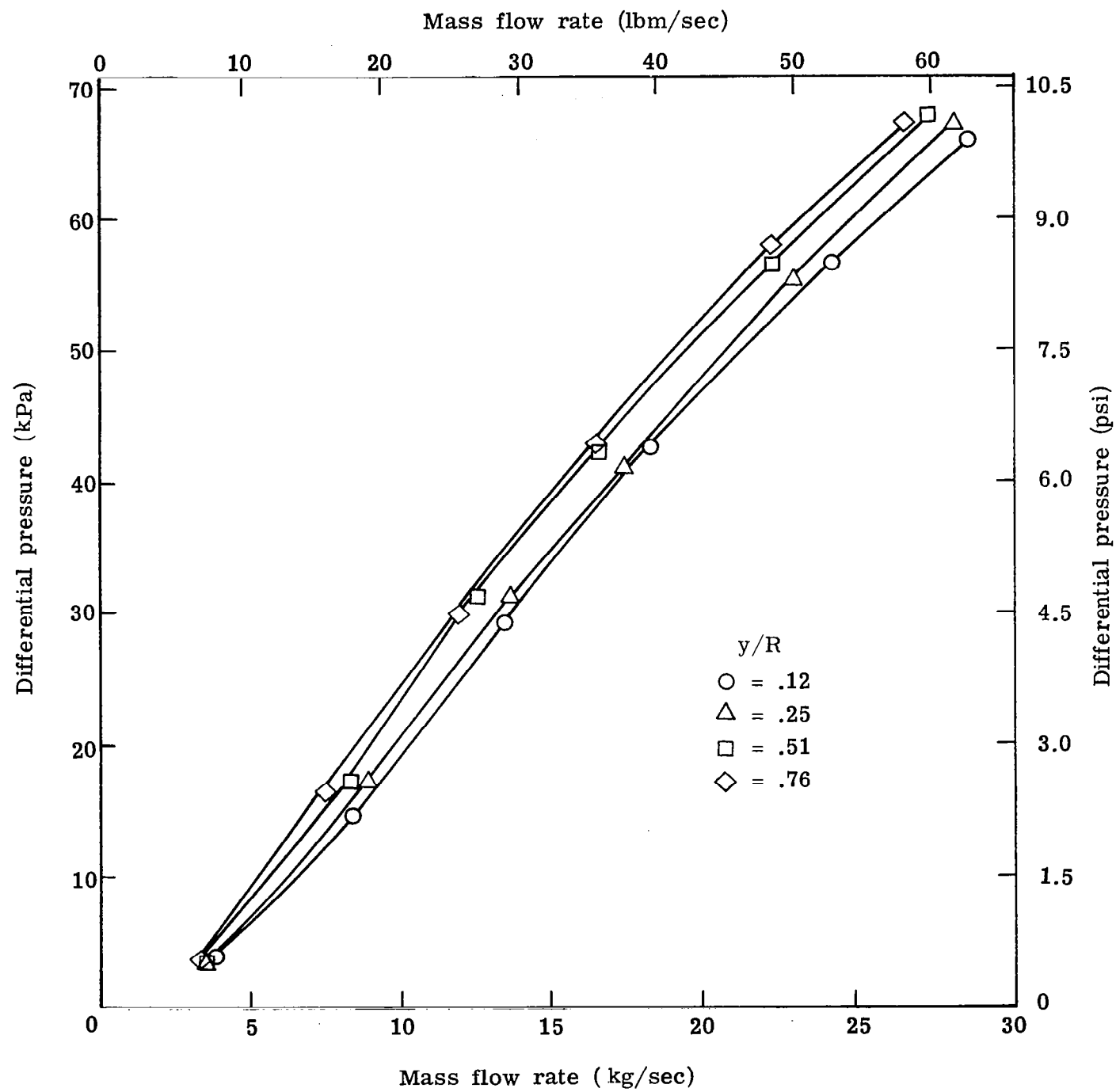


Figure 26.- Mass flow rate through the downstream porous "Rigimesh" plate at several radial locations.

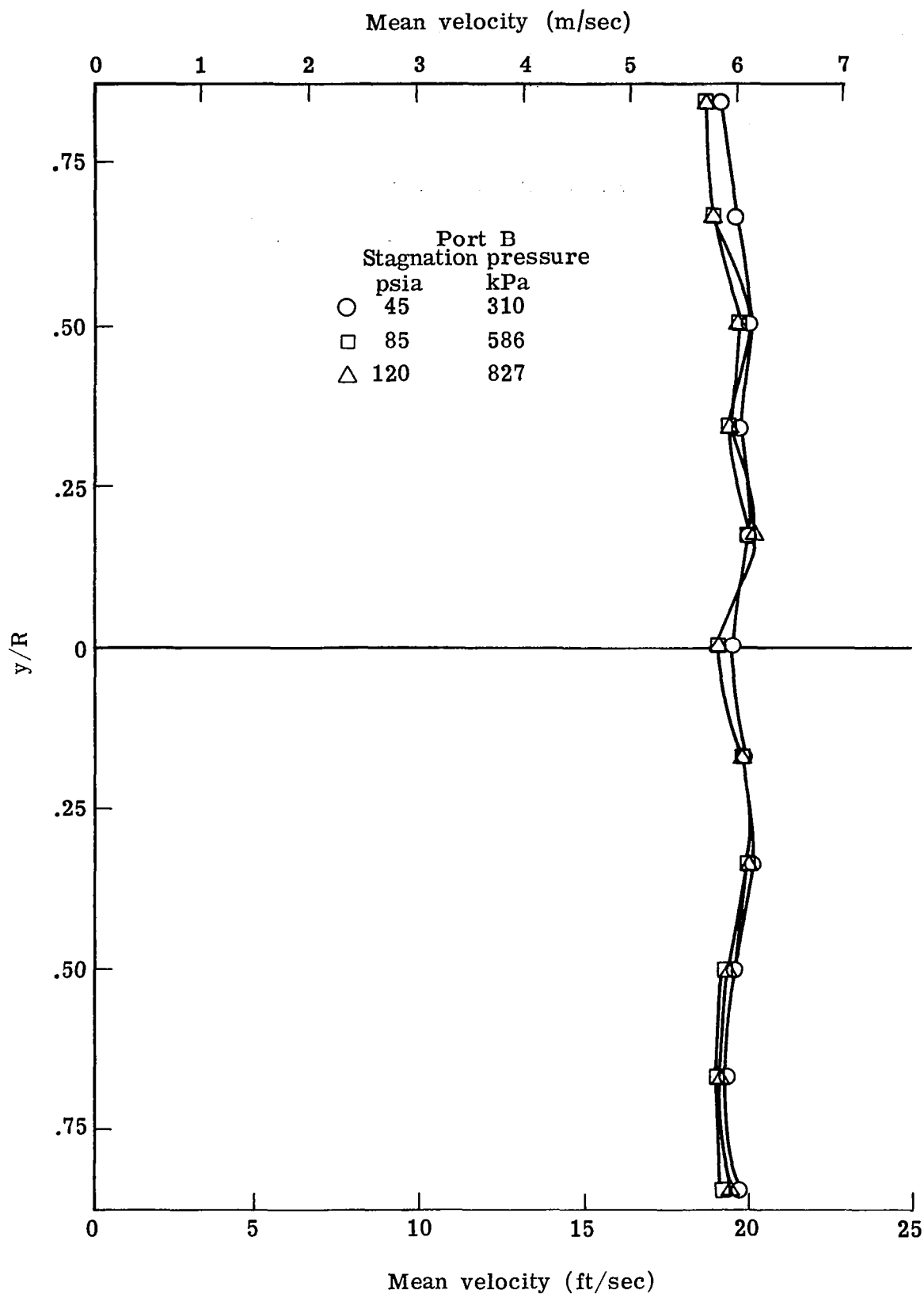


Figure 27.- Mean velocity profiles at Port B with the addition of a honeycomb-screen combination. (Downstream porous plate removed)

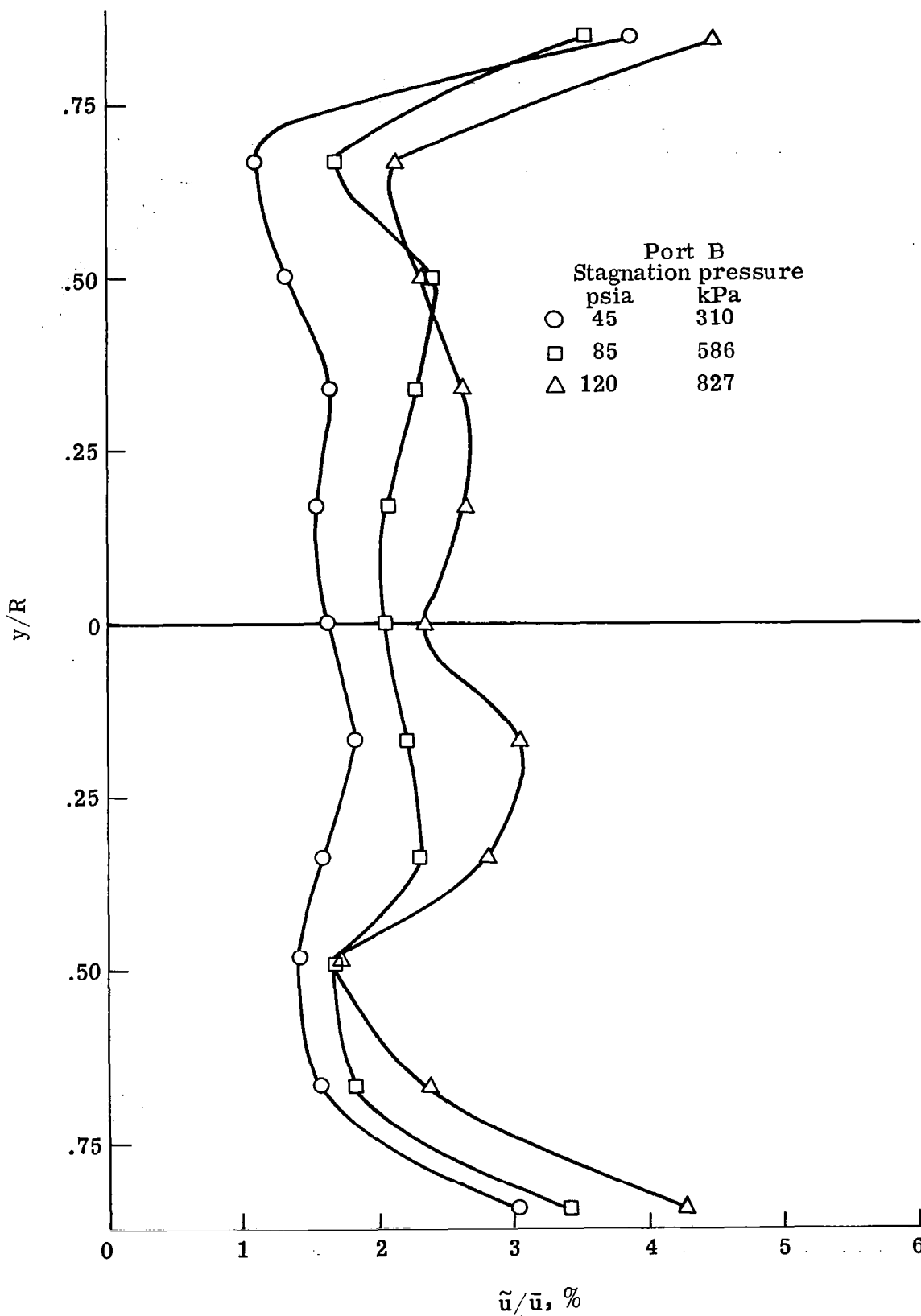


Figure 28.- Fluctuating velocity distributions at Port B with the addition of a honeycomb-screen combination. (Downstream porous plate removed)

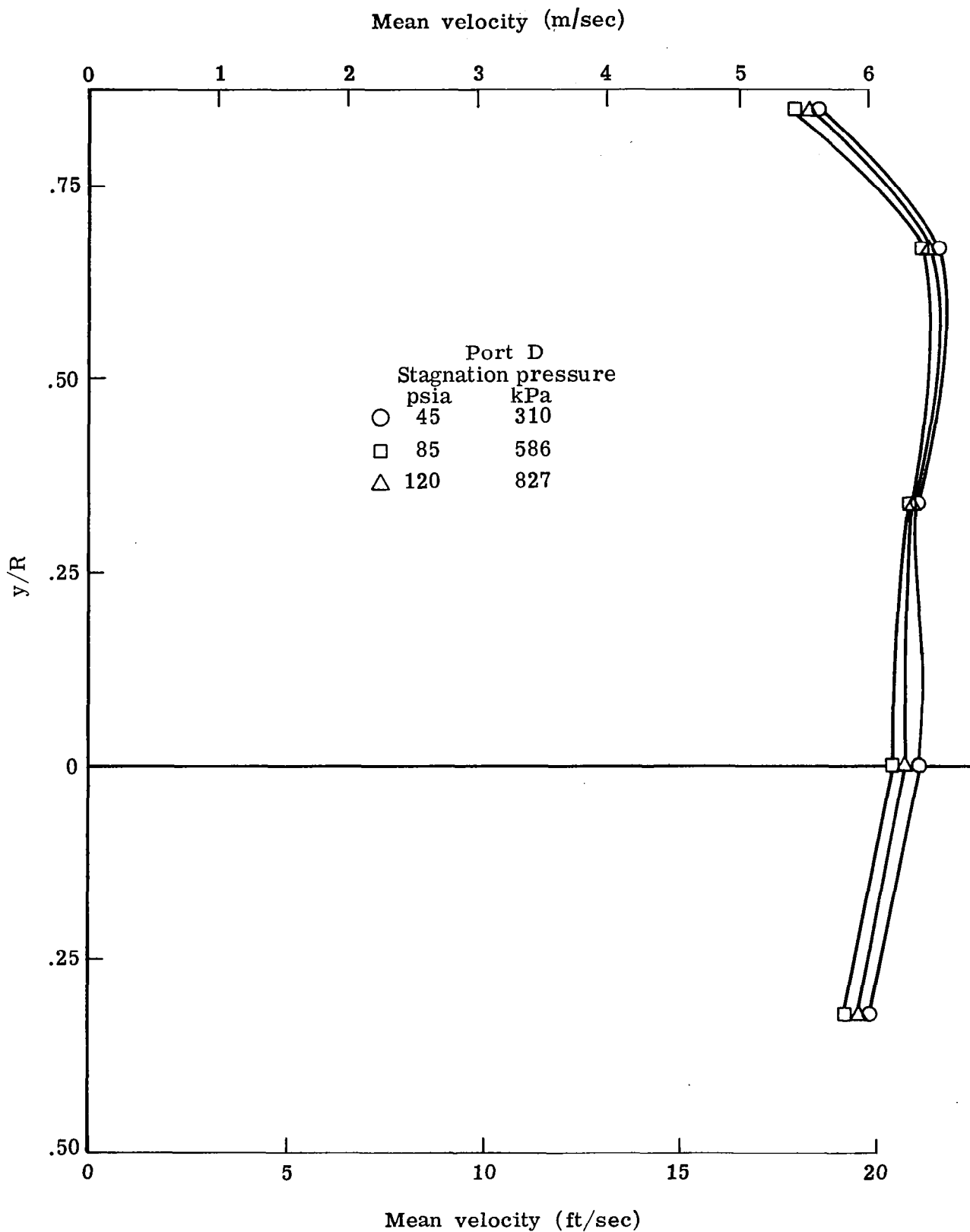


Figure 29.- Mean velocity profiles at Port D with the addition of a honeycomb-screen combination. (Downstream porous plate removed)

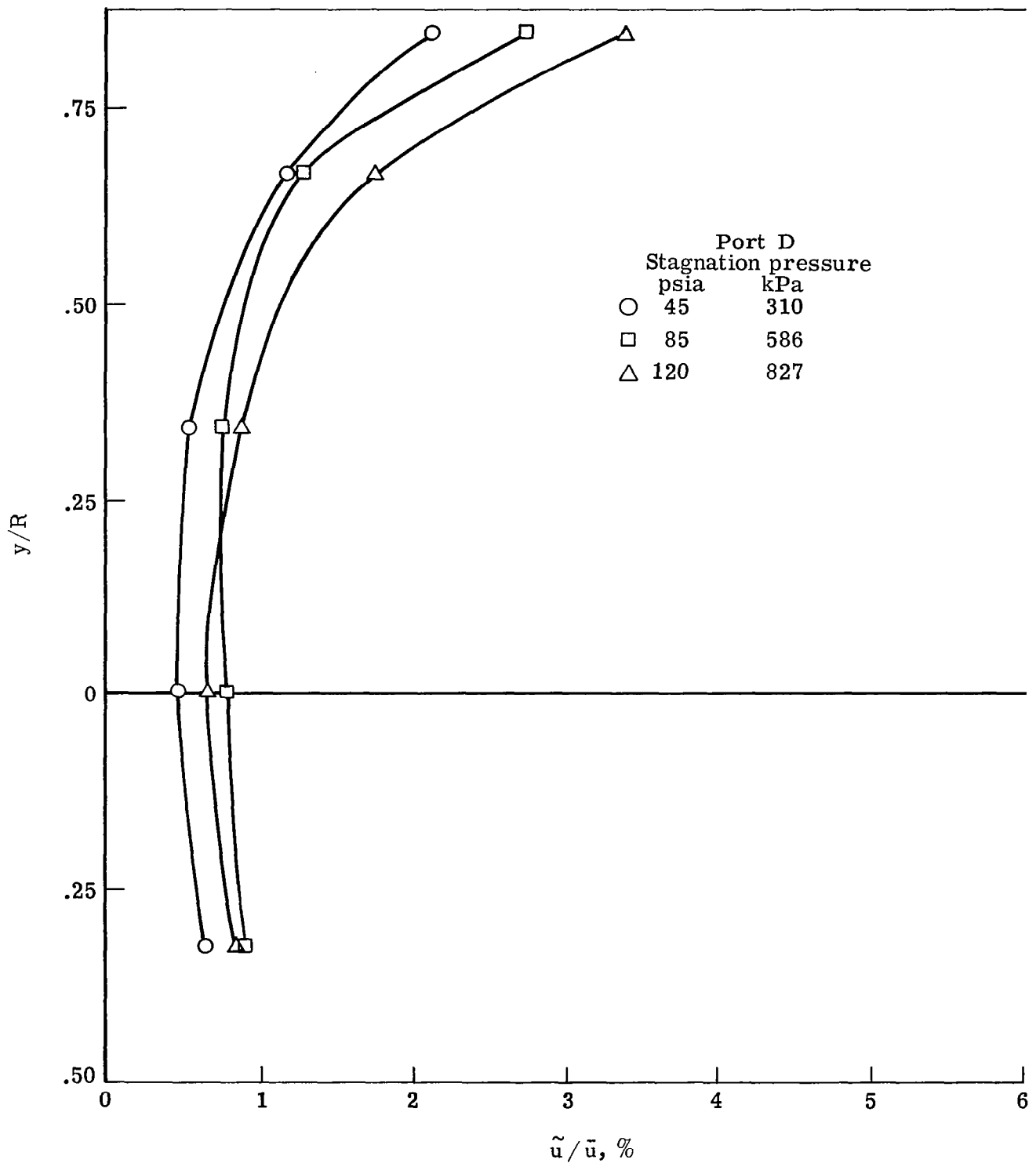


Figure 30.- Fluctuating velocity distributions at Port D with the addition of a honeycomb-screen combination. (Downstream porous plate removed)

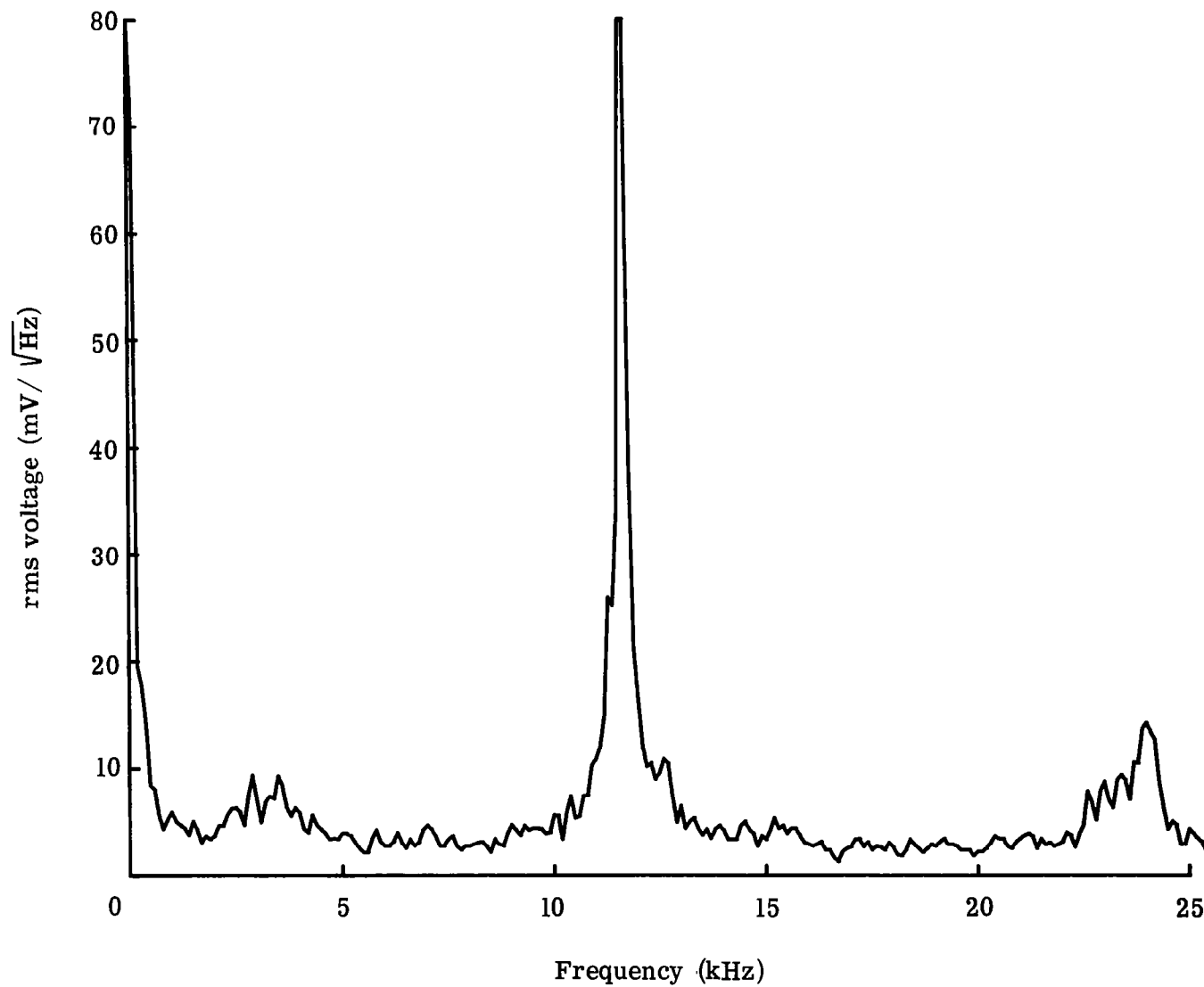


Figure 31.- Hot-wire spectra with a perforated plate in the chamber. Reynolds no./meter = 2.25×10^6 , Port B, $y/R = 0$.

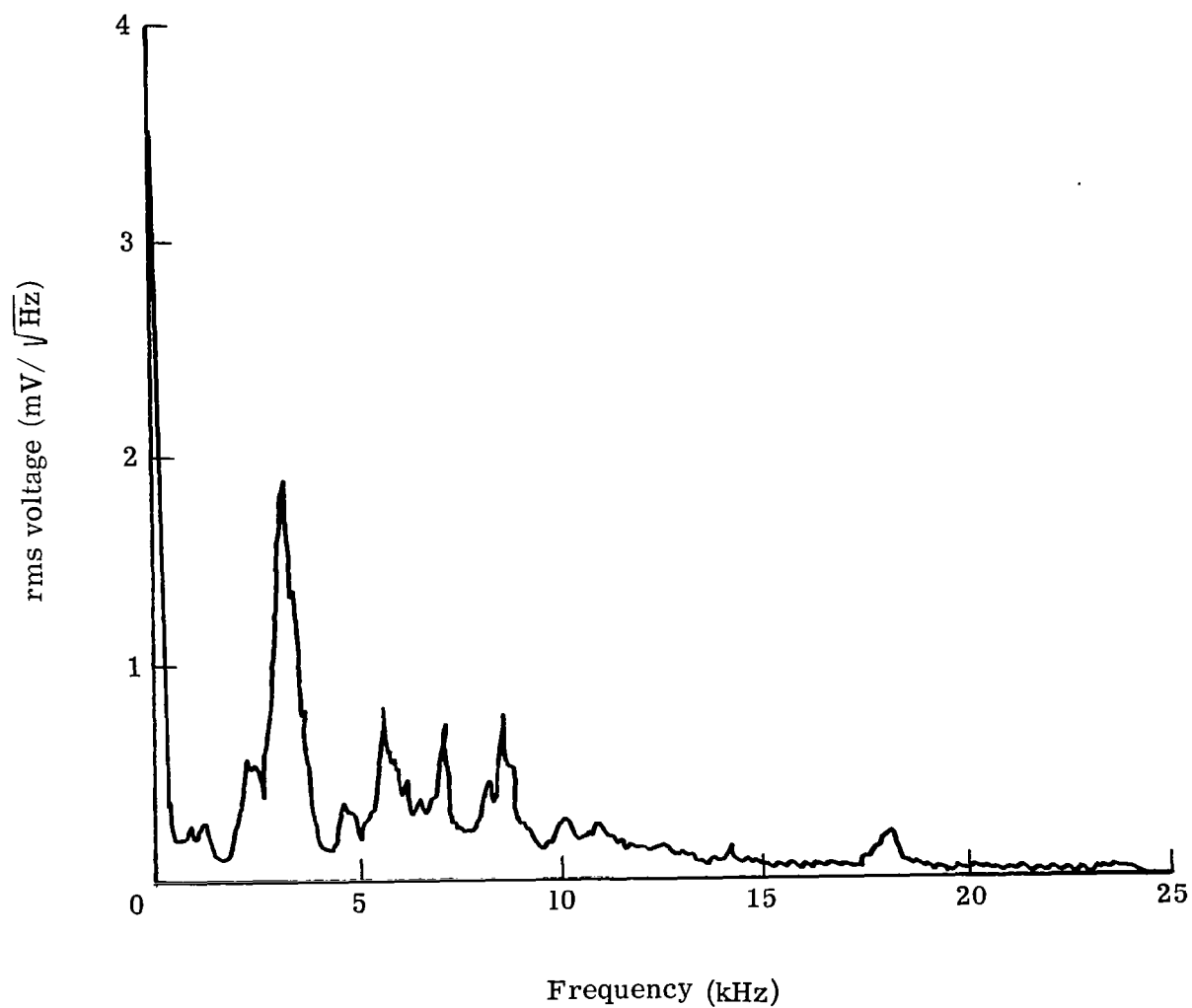


Figure 32.- Acoustic frequency spectra for flow at 61 m/sec through a straight orifice.

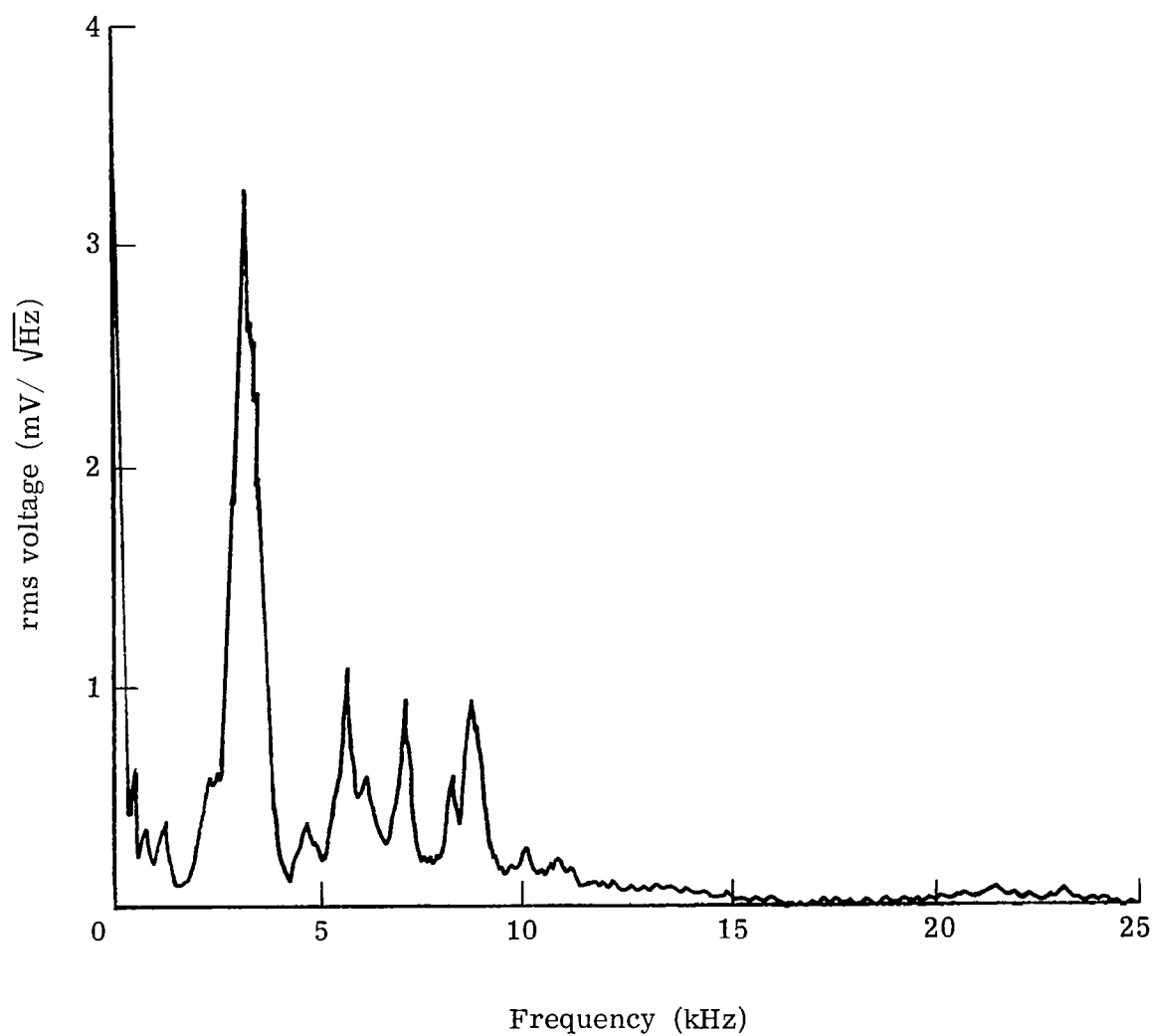


Figure 33.- Acoustic frequency spectra for flow at 61 m/sec through an orifice with an 82° included angle bevel on the upstream side.

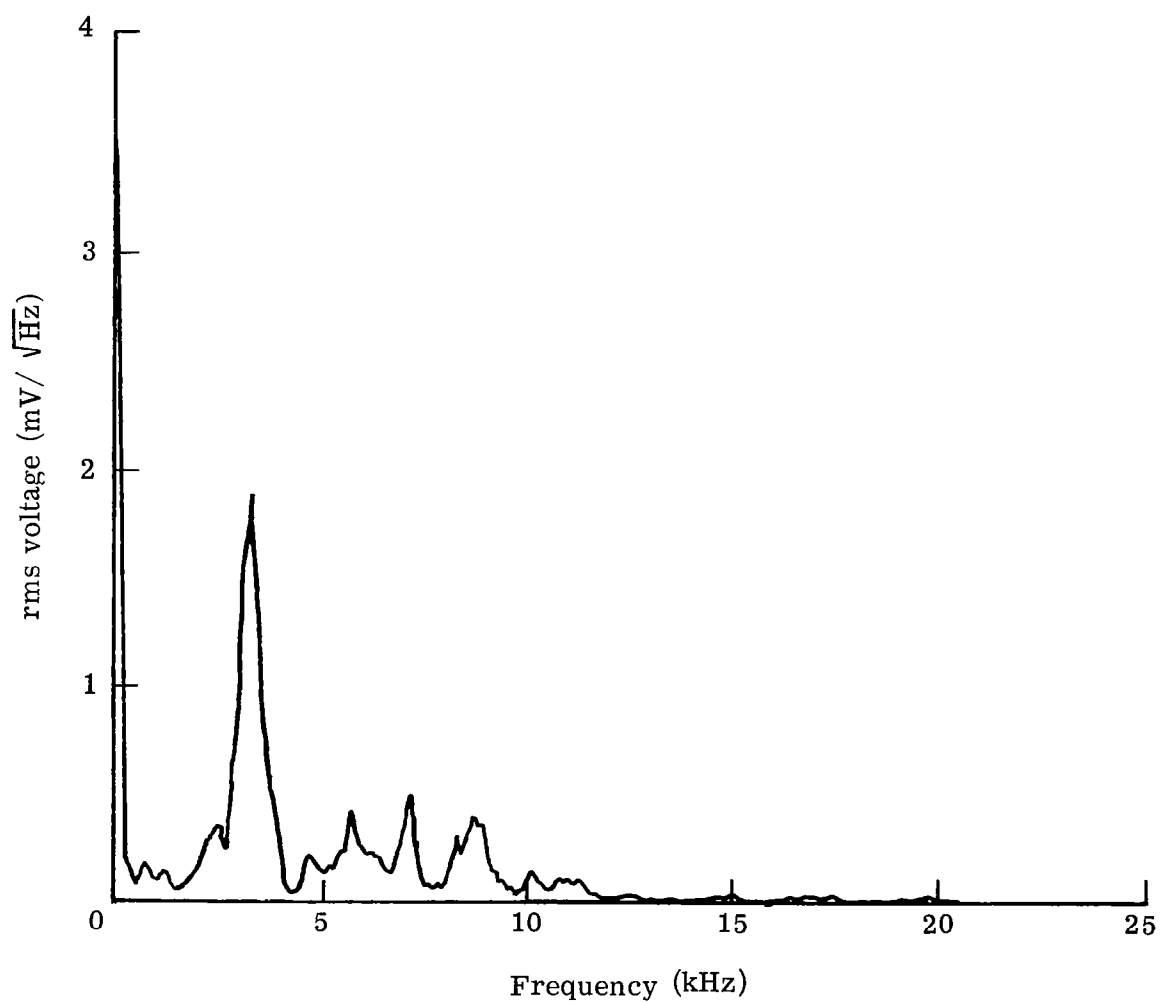


Figure 34.- Acoustic frequency spectra for flow at 61 m/sec through a straight orifice with screens attached to both sides of the orifice plate.

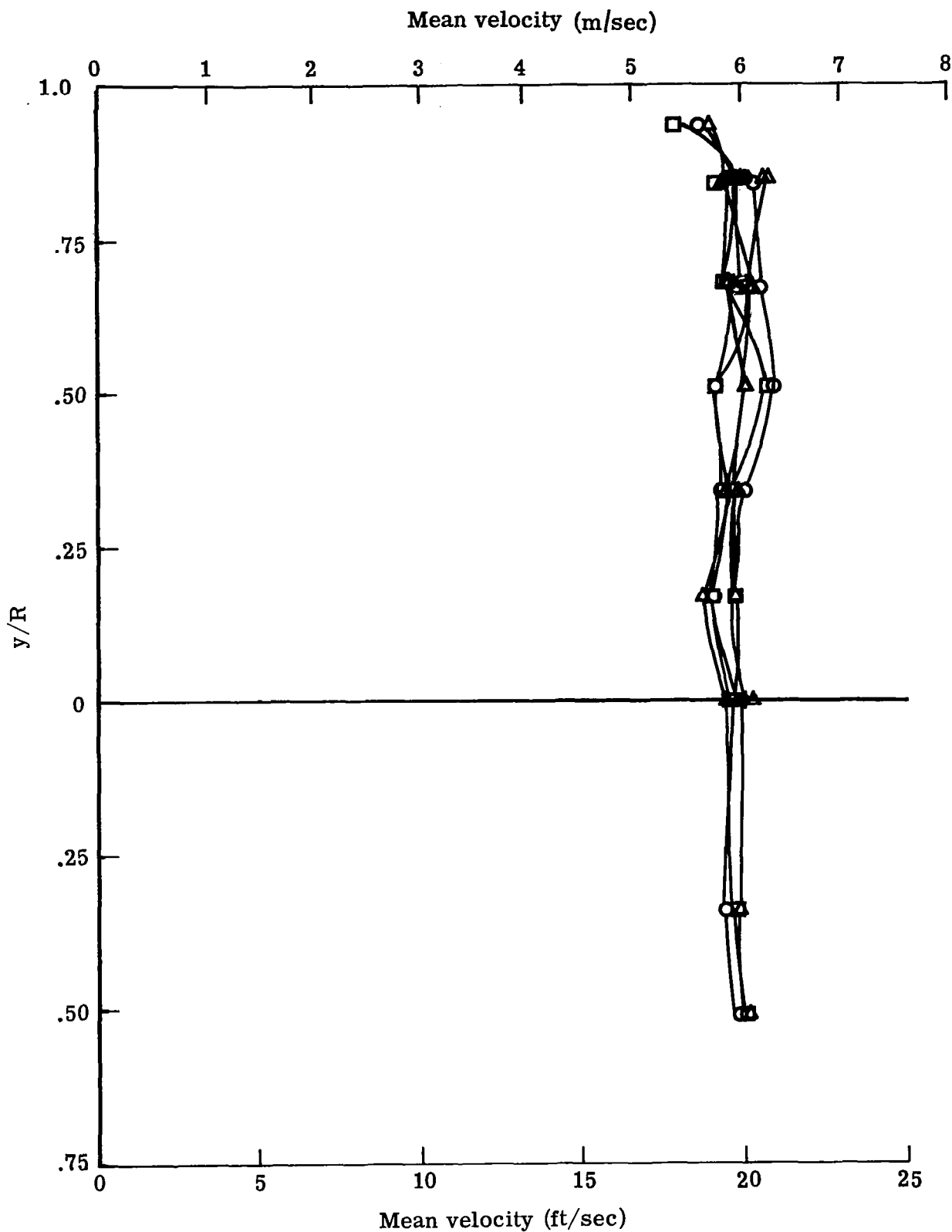


Figure 35.- Mean velocity profiles at port B with steel wool and downstream porous plate removed from the chamber.

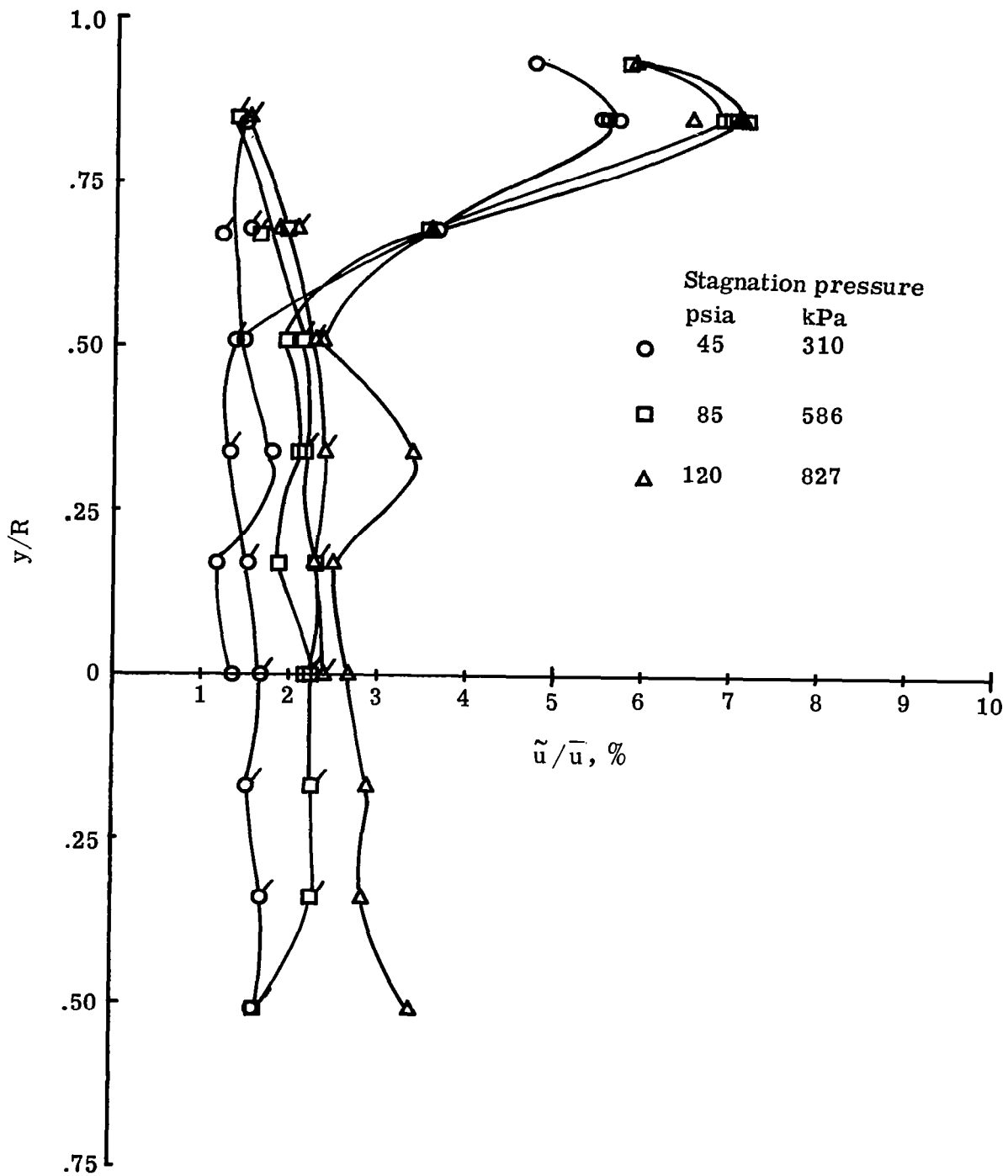


Figure 36.- Fluctuating velocity distributions at Port B with steel wool and downstream porous plate removed from the chamber.

1. Report No. NASA CR-3436		2. Government Accession No.		3. Recipient's Catalog No.	
4. Title and Subtitle AN EXPERIMENTAL INVESTIGATION OF A LARGE ΔP SETTLING CHAMBER FOR A SUPER- SONIC PILOT QUIET TUNNEL				5. Report Date June 1981	
				6. Performing Organization Code	
7. Author(s) Michael J. Piatt				8. Performing Organization Report No. R-SAL-03/81-03	
				10. Work Unit No.	
9. Performing Organization Name and Address Systems and Applied Sciences Corporation 17 Research Drive Hampton, Virginia 23666				11. Contract or Grant No. NAS1-16096	
				13. Type of Report and Period Covered Contractor Report	
12. Sponsoring Agency Name and Address National Aeronautics and Space Administration Washington, D.C. 20546				14. Sponsoring Agency Code 505-31-23-04	
15. Supplementary Notes Langley Technical Monitor: Ivan E. Beckwith Final Report					
16. Abstract This report is a study of the flow quality in the settling chamber of a blowdown supersonic pilot quiet tunnel. The mean streamwise flow distributions and turbulence levels across the chamber were measured with a hot wire anemometer downstream of a series of porous "Rigimesh" plates which have been shown to be an effective means of reducing the chamber acoustic disturbance levels due to upstream pipe and valve systems. Data presented shows that these plates can produce nonuniform mean flow distributions which result in the generation of large vorticity fluctuations. Tests made with various types of flow conditioners downstream of the porous plates showed that a series of screens was the most effective means of achieving the objective of a uniform mean flow distribution with reduced vorticity levels downstream of the porous components. Frequency spectra obtained across the series of screens show that they reduce vorticity over a wide frequency range for several different initial upstream vorticity conditions. The results indicate that improvements in the mechanical installation of the porous plates and damping screens and the use of porous plates with more uniform porosity should reduce the freestream velocity fluctuations to the minimum acoustic levels of about 0.5 percent.					
17. Key Words (Suggested by Author(s)) Turbulence levels Spectra Low-speed flow Acoustic attenuation			18. Distribution Statement Unclassified - Unlimited Subject Category 09		
19. Security Classif. (of this report) Unclassified	20. Security Classif. (of this page) Unclassified	21. No. of Pages 79	22. Price A05		